EG&G Idaho, Inc.

FORM EG&G-229
(Rev. 01-80)

**LOFT TECHNICAL REPORT**

| | |
|---|---|
| Title: LOFT LEAD ROD TEST RESULTS EVALUATION | LTR No. LO-87-80-138 |
| Author: W. E. DRISKELL AND E. L. TOLMAN | Released By LOFT CDCS |
| Performing Organization: LOFT MEASUREMENTS DIVISION | Date July 30, 1980 |
| LOFT Review and Approval: A. Ray 7-30-80 — M. L. Russell 7/23/80 — D. Hanson — [illegible] | Project System Engineer: R. E. Tiedt 7/8/80 |

FE&OB Mgr. | LIFB Mgr. | LMD Mgr. | LTSD Mgr.


The purpose for evaluating the LOFT Lead Rod Test (simulations of large break, loss-of-coolant accidents) data was to determine; (a) if the centerline thermocouple and fuel rod elongation sensor data show indications of the collapsed fuel rod cladding, (b) the capability of the FRAP-T5 computer code to accurately predict cladding collapse, and (c) if cladding surface thermocouples enhance fuel rod cooling. With consideration to unresolved questions on data integrity, it was concluded that:

(1) The fuel rod centerline thermocouple and elongation sensor data do show indications of the fuel rod cladding collapse,

(2) The FRAP-T5 code conservatively predicts cladding collapse, and

(3) There is an indication that cladding surface thermocouples are enhancing fuel rod cooling.


DISPOSITION OF RECOMMENDATIONS

No disposition required.

ABSTRACT

The purpose for evaluating the LOFT Lead Rod Test (simulations of large break, loss-of-coolant accidents) data was to determine; (a) if the centerline thermocouple and fuel rod elongation sensor data show indications of the collapsed fuel rod cladding, (b) the capability of the FRAP-T5 computer code to accurately predict cladding collapse, and (c) if cladding surface thermocouples enhance fuel rod cooling. With consideration to unresolved questions on data integrity, it was concluded that:

(1) The fuel rod centerline thermocouple and elongation sensor data do show indications of the fuel rod cladding collapse,

(2) The FRAP-T5 code conservatively predicts cladding collapse, and

(3) There is an indication that cladding surface thermocouples are enhancing fuel rod cooling.

## SUMMARY

An analysis of the LOFT Lead Rod Test data was completed to; (a) determine if the cladding elongation and fuel centerline temperature reflected cladding collapse, (b) determine the capability of the FRAP-T5 computer code to accurately predict cladding deformation and (c) determine if the hypothesized surface thermocouple effect could be identified by analyzing centerline temperature data.

The cladding elongation and fuel centerline temperature data obtained during the power ramp phase of each LOFT lead rod test were analyzed for significant changes after cladding collapse occurred. Detectable changes in these parameters would provide a method of identifying cladding deformation in LOFT fuel.

Evaluating the capability of the FRAP-T5 code to accuractely predict cladding deformation was done by comparing code calculated data with test data. Accurate prediction by the code would provide a method of assessing the condition of the LOFT fuel cladding and would provide a tool for LOFT fuel requalification.

The fuel centerline temperature response for rods with and without cladding surface thermocouples were analyzed to identify possible surface thermocouple effects that increase the rod cooling at the location of the thermocouples during loss-of-coolant transients. The relative magnitude and rate of change of the centerline temperature between two fuel rods were analyzed to identify possible increased cooling that could be related to the surface thermocouples.

The following is a summary of the results and conclusions of this posttest analysis:

1. The cladding elongation data obtained during power ramps show a significant offset in the elongation after cladding collapse occurred. Also an increase in the elongation was observed during the power ramp subsequent to cladding collapse. The data analysis, however, indicate that cladding elongation may be complicated by the number-of-ramps and rate-of-ramp dependence. Futhermore, cladding elongation appears to differ for different fuel rods. It is concluded that under controlled power ramp rates, cladding collapse can probably be detected through cladding elongation data. A careful and continuous monitoring will be required to assure that data are obtained before collapse for comparison with data obtained after collapse.

2. The comparison of fuel centerline temperatures before and after cladding collapse shows a reduction in the centerline temperature after collapse. Significant differences also occur in the centerline temperature from rod to rod. Therefore, detecting cladding deformation from centerline temperature data will require continuous monitoring and comparison of current data with the data from a previous test for each rod.

3. The comparison of calculated and measured transient centerline temperature data provides a basis for concluding that the FRAP-T5 calculated cladding collapse is conservatively predicted, i.e., the code predicts cladding collapse for less severe conditions of temperature and pressure than occurs in reality. Thus, the code would provide a conservative estimate of cladding collapse for LOFT core requalification.

4. It was concluded that a definite surface thermocouple effect cannot be established from centerline temperature data obtained during the LOFT lead rod tests. Abnormal centerline temperature data, which has not been explained, were observed for one fuel rod during one test. In

addition, there is evidence that one of the fuel rods received more coolant during two of the tests. The centerline temperature data obtained for fuel rods with and without surface thermocouples, however, do show a relative response that would be expected if the surface thermocouples had enhanced the rod cooling.

CONTENTS

FIGURES

TABLES

# 1. INTRODUCTION

The PBF/LOFT Lead Rod (LLR) series of tests[1,2] consisted of four tests that were conducted in the Power Burst Facility (PBF) at the Idaho National Engineering Laboratory during February 28 through May 18, 1979. The LLR tests were designed to simulate the cladding deformation conditions expected for the Loss-of-Flow Test (LOFT) Power Ascension Tests, which are a series of loss-of-coolant experiments (LOCEs). The objectives of the LLR tests were; (a) to experimentally determine the severity and extent of cladding deformation expected to occur during the LOFT LOCEs, (b) to evaluate the adverse effects of cladding deformation (collapse or waisting)[a] on the mechanical response during power operation after the LOCE, and (c) to provide a data base to evaluate the usefulness of the Fuel Rod Analysis Program Transient (FRAP-T) computer code in evaluating the condition of the LOFT core subsequent to a LOCE.

Pursuant to these test objectives, the purposes for the posttest analysis presented here were:

(1) Review the steady-state cladding elongation and fuel centerline temperature data to determine if changes in those data could be correlated to cladding deformation.

(2) Evaluate the capability of FRAP-T5 to calculate fuel centerline temperatures for fuel with collapsed cladding and operating at steady-state conditions.

---

a. Collapse refers to a uniform circumferential collapse of cladding onto the fuel pellet. Waisting refers to a plastic flow of the cladding into the small axial gaps between pellets.

(3) Evaluate the capability of FRAP-T5 to accurately predict cladding deformation and calculate fuel centerline temperatures during a LOCE.

In addition, the centerline temperature response from fuel rods with and without cladding surface thermocouples were reviewed to identify possible enhanced cooling caused by the surface thermocouples.

Results of this analysis are presented below in two categories; (a) steady-state analysis and (b) transient analysis. Included in this report are brief descriptions of the LLR test series (Section 2) and the FRAP-T5 computer code (Section 3) used for the calculations. Steady-state analysis of fuel centerline and cladding elongation data are presented in Section 4. Section 5 compares the results of transient calculations to the measured transient data and evaluates the transient centerline temperature responses for possible surface thermocouple effects. Finally, the results and conclusions are summarized in Section 6.

## 2. THE LLR TEST SERIES DESCRIPTION

The LLR test series consisted of four tests. These tests were designated LLR-3, LLR-5, LLR-4 and LLR-4A and were conducted in that order. Each test consisted of four fuel rods with each rod shrouded in a 1.613 cm ID tube which provided and independent coolant channel. Figure 1 is a cross section showing the LLR test configuration. The LLR test hardware was supported at the desired elevation within the PBF inpile tube by the hanger tube. The hanger tube also provided the flow channel for the reflood water. The fuel rods consisted of a 0.9144 m pellet stack of 93% theoretical density, 9.5 wt% enriched fuel, back filled with helium at atmospheric pressure and were typical of the LOFT fuel except in length, $UO_2$ enrichment and densification stability. (A list of the fuel rod parameters pertinent to these analysis, is provided in Table I). Seven fuel rods were utilized in the LLR test series. These rods were designated 312-1, 312-2, 312-3, 312-4, 345-1, 345-2 and 399-2. Figure 2 identifies the rods utilized in each test. During the first test, LLR-3, fuel rods 312-1 and 312-2 were encased in Zircaloy-4 shrouds whereas rods 312-3 and 312-4 were encased in stainless steel shrouds. The stainless steel shrouds were designed to reduce the enclosed test rod power by approximately 13% to simulate power levels on the periphery of the LOFT core. Rod 312-3 failed during test LLR-3 as a result of water logging and consequently the failed rod and the other low power rod, rod 312-4, were removed following the test. These low power rods were replaced with rods 345-1 and 345-2 having Zircaloy-4 shrouds. Thus for tests LLR-5, LLR-4, and LLR-4a the power for the four test rods was essentially the same during any test. Fuel rod 312-1 was removed after test LLR-4 for post irradiation examination (PIE) and replaced with rod 399-2.

Each test was characterized by several phases, including: (a) ramping to power and power calibration, (b) steady-state operation to precondition the fuel and build up fission product inventory, (c) system blowdown and (d) system reflood and fuel rod quench.

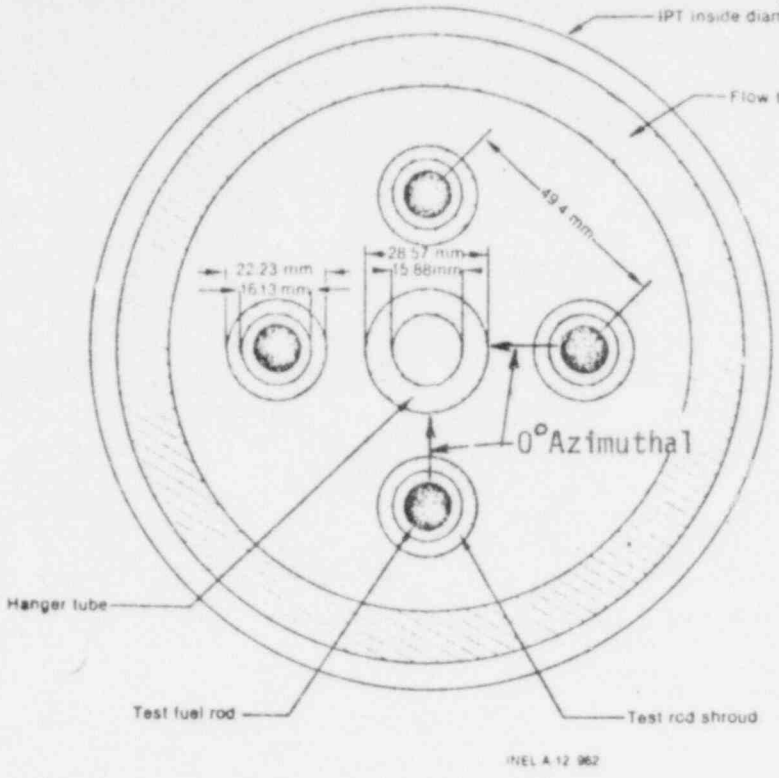


Figure 1 PBF/LOFT lead rod test geometry.

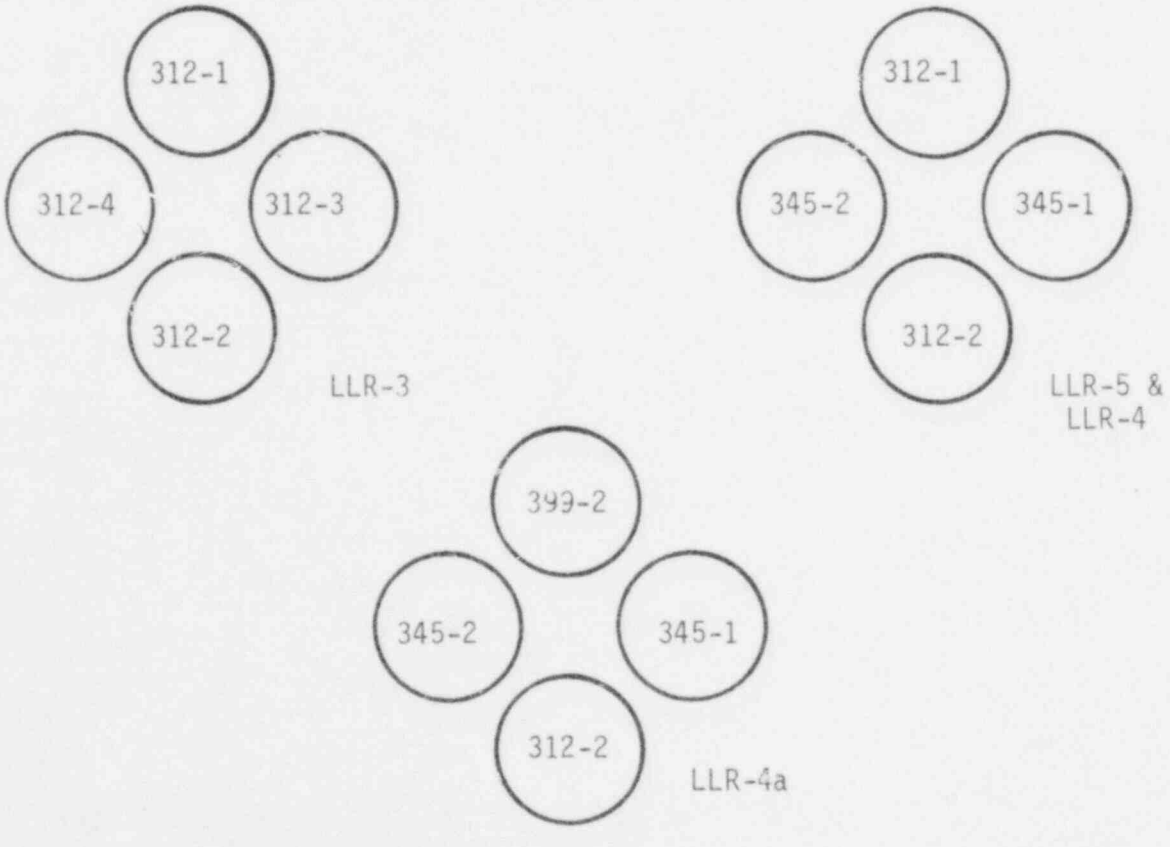


Figure 2 PBF/LOFT lead rod tests and corresponding fuel rods.

TABLE I

THE FRAP-T5 COMPUTER PROGRAM INPUT FOR THE
POSTTEST ANALYSES OF THE PBF/LOFT LEAD ROD TESTS

| | LLR | LOFT* |
|---|---|---|
| Pellet Diameter, cm | 0.9294 | .929 |
| Pellet Length, cm | 1.524 | 1.524 |
| Pellet Total Dish Volume, cc | 0.019 | 0.019 |
| $UO_2$ Density, % TD | 93.0 | 92.4 |
| Pellet Stack Length, m | 0.9144 | 1.6767 |
| Cladding OD, cm | 1.0719 | 1.0719 |
| Cladding ID, cm | 0.9484 | 0.9484 |
| Cladding Cold Work | 0.2 | 0.1 |
| Axial Peak/Average Power Density | 1.345 | 1.621 |
| Fuel Densification Stability** | 1.0 | 3.5 |

Code Options:

1. Coleman pellet relocation correlation
2. Modified Ross and Stoute gap conductance

* Included for comparison

** Percent increase in density after resintering at 1700C for 24 hrs.

The power calibration phase consisted of calculating the fuel rod average power based on measured flow and the differential inlet-outlet coolant temperatures. The rods were ther preconditioned for two to three hours at the peak power levels specified for the test. Following the precondition phase, the LOCE was initiated by opening high speed valves in the cold leg simulating a 200% doubled-ended cold leg break.

The fuel rod instrumentation for the LLR tests consisted of thermocouples to measure cladding surface temperature and fuel centerline temperature, and linear variable differential transformers to measure changes in the axial length of each rod. Instruments were also included to measure the pressure, temperature and flow rate of the coolant in each flow shroud. The type and location of instruments whose data were pertinent to the analysis presented in this report are listed in Table II. Included in the table is the type of qualification given the preblowdown data (power calibration and steady-state) and the blowdown data (blowdown and reflood) taken during each LOCE. Three types of qualification were applied to the data; (a) qualified, (b) trend, and (c) restricted. Definitions are provided in Table II.

TABLE II

PBF/LOFT LEAD ROD DATA PRESENTATION AND QUALIFICATION[1] -
DATA CONSIDERED IN POSTTEST ANALYSES

| Measurement | | LLR-3 | | LLR-5 | | LLR-4 | | LLR-4a | |
|---|---|---|---|---|---|---|---|---|---|
| Rod | Location | Pre-Blowdown | Blowdown | Pre-Blowdown | Blowdown | Pre-Blowdown | Blowdown | Pre-Blowdown | Blowdown |
| **Fuel Centerline Temperature** | | | | | | | | | |
| 312-1 | 0.533 m elev. | Trend | Trend | Trend | Trend | Trend | Trend | -- | -- |
| 312-2 | 0.457 m elev. | Trend | Trend | Trend | Trend | Trend | Trend | Trend | Trend |
| 312-3 | 0.533 m elev. | Failed | Failed | -- | -- | -- | -- | -- | -- |
| 312-4 | 0.533 m elev. | Trend | Failed | -- | -- | -- | -- | -- | -- |
| 345-1 | 0.533 m elev. | -- | -- | Qualified | Qualified | Qualified | Qualified | Qualified | Qualified |
| 345-2 | 0.457 m elev. | -- | -- | Qualified | Qualified | Qualified | Qualified | Qualified | Qualified |
| 399-2 | 0.457 m elev. | -- | -- | -- | -- | -- | -- | Qualified | Failed |
| **Cladding Surface Temperature** | | | | | | | | | |
| 312-1 | 0.533 m elev. 180° azimuth. | Qualified | Qualified | Qualified | Qualified | Qualified | Qualified | -- | -- |
| 312-1 | 0.533 m elev. 0° azimuth. | Qualified | Qualified | Qualified | Qualified | Qualified | Qualified | -- | -- |
| 312-2 | 0.533 m elev. 180° azimuth. | Qualified | Qualified | Qualified | Qualified | Qualified | Qualified | Qualified | Qualified |

TABLE II (Continued)

| Measurement | | LLR-3 | | LLR-5 | | LLR-4 | | LLR-4a | |
|---|---|---|---|---|---|---|---|---|---|
| Rod | Location | Pre-Blowdown | Blowdown | Pre-Blowdown | Blowdown | Pre-Blowdown | Blowdown | Pre-Blowdown | Blowdown |
| Cladding Surface Temperature (Continued) | | | | | | | | | |
| 312-2 | 0.457 m elev. 0° azimuth. | Qualified | Qualified | Qualified | Qualified | Qualified | Qualified | Qualified | Qualified |
| 312-3 | 0.533 m elev. 180° azimuth. | Qualified | Qualified | -- | -- | -- | -- | -- | -- |
| 312-3 | 0.533 m elev. 0° azimuth. | Qualified | Qualified | -- | -- | -- | -- | -- | -- |
| 312-4 | 0.533 m elev. 180° azimuth. | Qualified | Qualified | -- | -- | -- | -- | -- | -- |
| 312-4 | 0.533 m elev. 0° azimuth. | Qualified | Qualified | -- | -- | -- | -- | -- | -- |
| 345-1 | 0.533 m elev. 180° azimuth. | -- | -- | Qualified | Qualified | Qualified | Qualified | Qualified | Qualified |
| 345-1 | 0.533 m elev. 0° azimuth. | -- | -- | Qualified | Qualified | Qualified | Qualified | Qualified | Qualified |
| 399-2 | 0.533 m elev. 180° azimuth. | -- | -- | -- | -- | -- | -- | Qualified | Qualified |
| 399-2 | 0.533 m elev. 0° azimuth. | -- | -- | -- | -- | -- | -- | Qualified | Qualified |

TABLE II (Continued)

| Measurement | | LLR-3 | | LLR-5 | | LLR-4 | | LLR-4a | |
|---|---|---|---|---|---|---|---|---|---|
| Rod | Location | Pre-Blowdown | Blowdown | Pre-Blowdown | Blowdown | Pre-Blowdown | Blowdown | Pre-Blowdown | Blowdown |
| **Cladding Elongation (LVDT)** | | | | | | | | | |
| 312-1 | | Restrained[a] | Trend | Restrained | Trend | Restrained | Trend | -- | -- |
| 312-2 | | Restrained | Trend | Restrained[c] | Trend | Failed | Trend | Restrained | Trend |
| 312-3 | | Restrained | Trend | -- | -- | -- | -- | -- | -- |
| 312-4 | | Restrained[b] | Trend | -- | -- | -- | -- | -- | -- |
| 345-1 | | -- | -- | Restrained | Trend | Restrained | Trend | Failed | Trend |
| 345-2 | | -- | -- | Restrained | Trend | Restrained | Trend | Failed[d] | Failed |
| 399-2 | | -- | -- | -- | -- | -- | -- | Trend | Trend |
| **Core Pressure** | | | | | | | | | |
| | Top Support Plate | Qualified | Qualified | Trend | Trend | Qualified | Trend | Qualified | Qualified |
| **Coolant Volumetric Flow** | | | | | | | | | |
| 312-2 | Inlet | Qualified | Restrained | Qualified | Restrained | Qualified | Restrained | -- | -- |
| 345-1 | Inlet | -- | -- | Qualified | Restrained | Qualified | Restrained | Qualified | Restrained |
| 345-1 | Outlet | -- | -- | Qualified | Restrained | Qualified | Restrained | Qualified | Restrained |
| 345-2 | Inlet | -- | -- | Trend | Failed | Failed | Failed | Qualified | Restrained |
| 345-2 | Outlet | -- | -- | Qualified | Restrained | Qualified | Restrained | Qualified | Restrained |

TABLE II (Continued)

| Measurement | | LLR-3 | | LLR-5 | | LLR-4 | | LLR-4a | |
|---|---|---|---|---|---|---|---|---|---|
| Rod | Location | Pre-Blowdown | Blowdown | Pre-Blowdown | Blowdown | Pre-Blowdown | Blowdown | Pre-Blowdown | Blowdown |
| Inlet Temperature | | | | | | | | | |
| 312-2 | Shroud Inlet | __ | Qualified | __ | Qualified | __ | Qualified | __ | Qualified |
| 345-1 | Shroud Inlet | -- | -- | __ | Qualified | __ | Qualified | __ | Qualified |

Notation:

Restrained - Data is considered correct but no comparable data exists.

Trend - Direction and time of deflection are considered correct but magnitude is questionable.

-- Not in service for this test.

__ No qualification given.

a. Data exhibits a changing zero base.

b. Data is associated with high frequency noise.

c. Data exhibits an instantaneous change in the zero base.

d. Data from this LVDT appears to be correct.

## 3. FRAP-T5 DESCRIPTION AND CALCULATIONAL METHOD

Calculations for the LLR posttest annalyses were done using the Fuel Rod Analysis Program-Transient, version 5[3] (FRAP-T5)[a]. FRAP-T5 is a FORTRAN IV computer code that predicts the transient response of light water reactor fuel during accident situations. Accidents that can be analyzed by FRAP-T5 may range from minor operational accidents to design basis accidents such as the loss-of-coolant accident.

FRAP-T5 is a multi-node (up to 20 nodes in both the radial and axial dimensions) code that calculates the mechanical and thermal fuel rod response given the time dependent fuel rod power and coolant boundary conditions. Included in the calculated parameters are; (a) temperature at each axial and radial node, (b) internal fuel rod pressures and (c) cladding deformation. The phenomena modeled by the code includes; (a) heat conduction, (b) elastic-plastic fuel and cladding deformation, (c) fuel-cladding mechanical interaction, (d) fission gas release, (e) transient fuel rod gas pressure, (f) heat transfer between fuel and cladding, (g) cladding oxidation, (h) cladding annealing, and (i) heat transfer from cladding to coolant. The code contains all the needed material properties[4], water properties[5], and heat transfer correlations.

FRAP-T5 has several built in user options. Included in these options is the ability to select gap conductance and fuel pellet conductivity models. For the calculations presented here, the modified Ross-Stoute gap conductance model in conjunction with the Coleman pellet relocation model were specified as suggested in code assessment studies[6]. (These models are defined in Reference 3.)

FRAP-T5 also has a restart option that allows the user to either continue a transient calculation or to perform additional calculations that

---

a. Configuration Control Number H0005838.

consider accumulative effects of previous calculations. Calculations for the LLR posttest analyses, except those involving fresh unirradiated fuel, were accomplished using the restart option. Thus, changes in the fuel rod geometry, such as cladding collapse, which were calculated to occur during a transient would be passed on to the next calculation. Transient calculations for fresh, unirradiated fuel were initiated from nominal beginning of life (BOL) fuel dimensions shown in Table I. The transient cladding surface temperature calculated by the code was forced to be equal to the measured temperature by inputting the measured temperature as the bulk coolant temperature in conjunction with large surface heat transfer coefficients. From the following surface heat transfer equation, it can be seen that by making the heat transfer coefficient (hs) arbitrarily large, the calculated cladding surface temperature ($T_c$) becomes essentially equal to the bulk coolant temperature ($T_b$):

$$q = \frac{h}{A} (T_c - T_b)$$

or

$$\frac{qA}{h} + T_b = T_c$$

By doing the transient calculations in this manner, it was possible to eliminate the uncertainties associated calculating coolant conditions and heat transfer coefficients.

For the power ramping or steady-state calculations, the cladding surface temperatures were calculated by the code based on the coolant inlet condition and mass flow together with the heat transfer logic within the code. The manner in which FRAP-T5 was used, i.e., whether the code was restarted from end-of-test conditions from a previous calculation or initiated from the BOL conditions is included in the discussion for each calculation.

# 4. STEADY-STATE ANALYSIS

Steady-state analysis included the comparison of the cladding elongation and the fuel centerline temperature data from test to test to determine if these data reflected the cladding deformation and consequently provide a method of detecting deformation in the LOFT fuel. In this regard, it was postulated that cladding deformation would increase the pellet-to-cladding interaction (PCI), which would result in greater cladding elongation on subsequent power operation. Also, cladding deformation would result in an increase in the gap conductance and consequently a decrease in the centerline temperature.

In addition, the steady-state analysis included an evaluation of the capability of FRAP-T5 to calculate fuel centerline temperatures with and without collapsed cladding. The steady state analysis is presented in two categories; (a) fuel rod elongation and (b) fuel centerline temperatures.

## 4.1 Cladding Elongation

Cladding elongation measurements made during the LLR test series were obtained from linear variable differential transformers (LVDTs). LVDTs are inductance coil devices consisting of a primary and two secondary windings. An alternating current is supplied to the primary, which induces a voltage in each secondary coil. The relative voltage induced in each is proportional to the location of a movable ferromagnetic core that is attached to the fuel rod. Differences in the voltage between the secondary coils provide the output signal, which is calibrated to give fuel rod elongation. For the LLR tests, the ferromagnetic core was attached to the lower end of the fuel rod and the body of the LVDT was attached to the inside of an extension to the fuel rod flow shroud. Because of this design characteristic, the LVDT measures the relative change in fuel rod and shroud length and an increase in shroud temperature (or length) would

result in an apparent decrease in fuel rod length. In addition to changes in shroud length, there are other factors limiting the accuracy of the LVDT. Among these other factors are temperature and ambient pressure. However, since temperature and pressure at the location of the LVDT were relatively constant during power ramps, the effect of these parameters is not considered.

The effect of the shroud elongation on the LVDT response is small for the data reviewed and therefore no correction to the LVDT data for this analysis was made. During power ramps, the temperature of the fuel rod coolant at any axial elevation is dependent on the power level. Since the coolant is in contact with the shroud, the temperature of the shroud is also dependent on power. A review of the shroud temperature data show the maximum increase in shroud temperature would be 15 K for a fuel rod average power of 40 KW/m. A 15 K increase in the temperature of the shroud would result in approximately 0.07 mm increase in the shroud length. Thus, the fuel rod elongation data presented in Figures 3, 4, 5, and 6 should have been increase by 0.07 mm at 40 kW/m and by lesser amounts for lower power levels. These small corrections to the data would neither significantly change the data base nor alter the conclusions made.

Cladding elongation data obtained during the power ramp for the LLR-3 test is shown in Figure 3 for rod 312-2 (a high power rod). Data from only this rod was selected because of an intermittent shift in the LVDT zero reading from the other high power rod (rod 312-1). In general the elongation data for the low power rod 312-2 followed the same trends as the data in Figure 3. The elongation, however, was less, which is probably indicative of the lower power. The elongation data for the other low power rod, rod 312-4, contained high frequency noise and was not considered. As indicated by the data in Figure 3, the power ramping and fuel conditioning phases for the LLR-3 test consisted of four significant power ramps. The first three resulted in successively larger power levels, as shown by the rod average power data included in Figure 3. The fourth ramp brought the

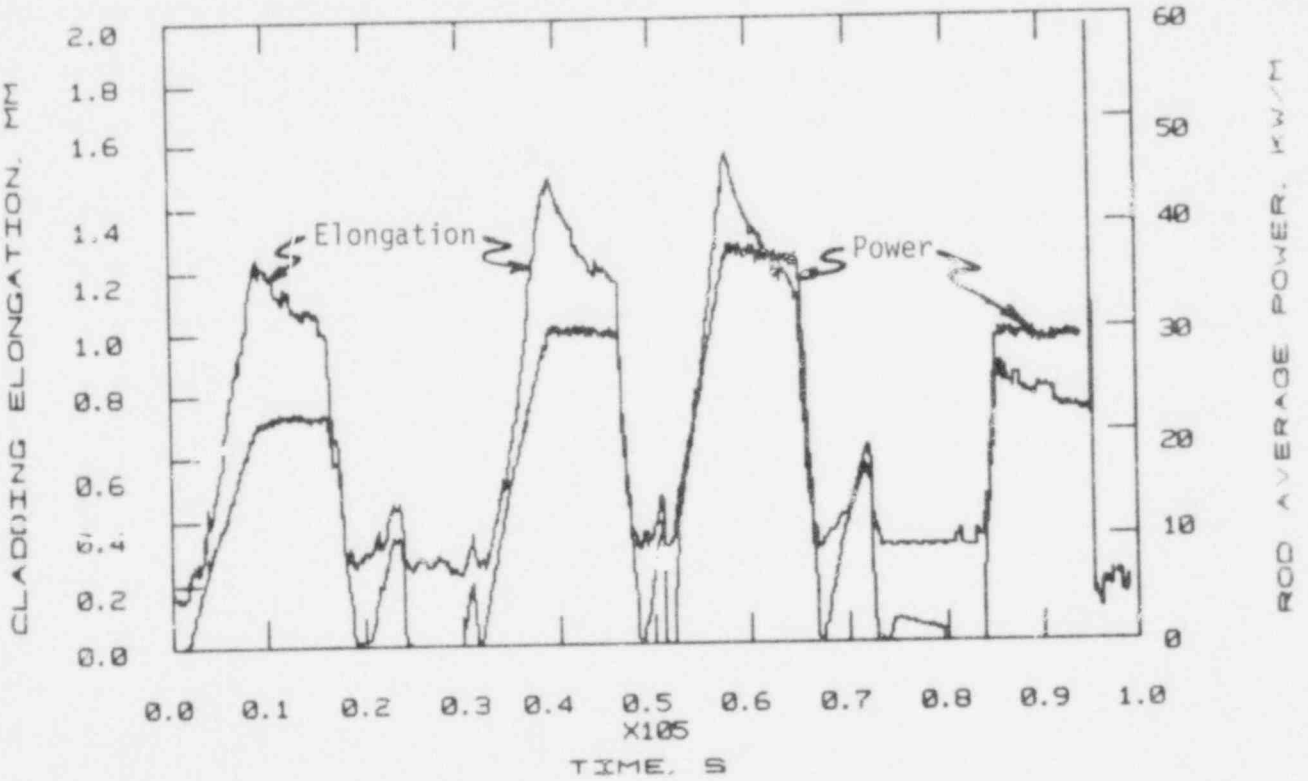


Figure 3 Fuel rod 312-2 average linear heat rate and cladding elongation measured during the LLR-3 power ramp.

power to the desired level for the LLR-3 test. From the data in Figure 3, it is noted that although the cladding elongation increases for each of the first three successive ramps, the elongation at any given power level becomes less with each power ramp. A different illustration of this is provided by Figure 4 where the cladding elongation data are plotted as a function of the rod average linear heat rate for each of the first three power ramps. Included in Figure 4 are unrestricted (free) thermal expansion for the cladding and fuel pellet stack calculated by FRAP-T5. As these data show, the cladding elongations measured during the power ramps are considerably greater (up to 8 times) than the free thermal expansion calculated for the cladding. Elongation measurements greater than the free thermal expansion of the cladding are common observations[7,8] and are attributed to pellet cracking and relocation resulting in pellet-cladding interaction (PCI). Since pellet cracking occurs at very low powers, it is postulated that sufficient PCI occurs early in the power ramps to result in the observed elongation. It is noted that all measured data in Figure 4 are less than the calculated free thermal expansion for the pellet stack.

The reduction in the cladding elongation for each successive power ramp (refer to Figure 4) has also been observed in previous tests[8]. where the phenomenon was attributed to fuel creep enhanced by a compressive load from the cladding, which reduces the PCI. A similar or closely related phenomenon would also explain the reduction in the elongation observed during periods of constant power as shown in Figure 3. A decrease in the elongation during periods of constant power suggests less elongation would be observed if the time to attain a certain power level were increased, i.e., a ramp rate dependence. Power ramps for the tests subsequent to LLR-3 were completed over longer periods of times or with smaller ramp rates. Effective ramp rates for each test, including the first three ramps for test LLR-3, were determined and are presented in Table III. The data in the table show the ramp rates for LLR-3 ranged from 2.1 to 4.8 times greater than the ramps for tests LLR-5, LLR-4 and LLR-4a. The data from test LLR-5, when compared with the first ramp data from test

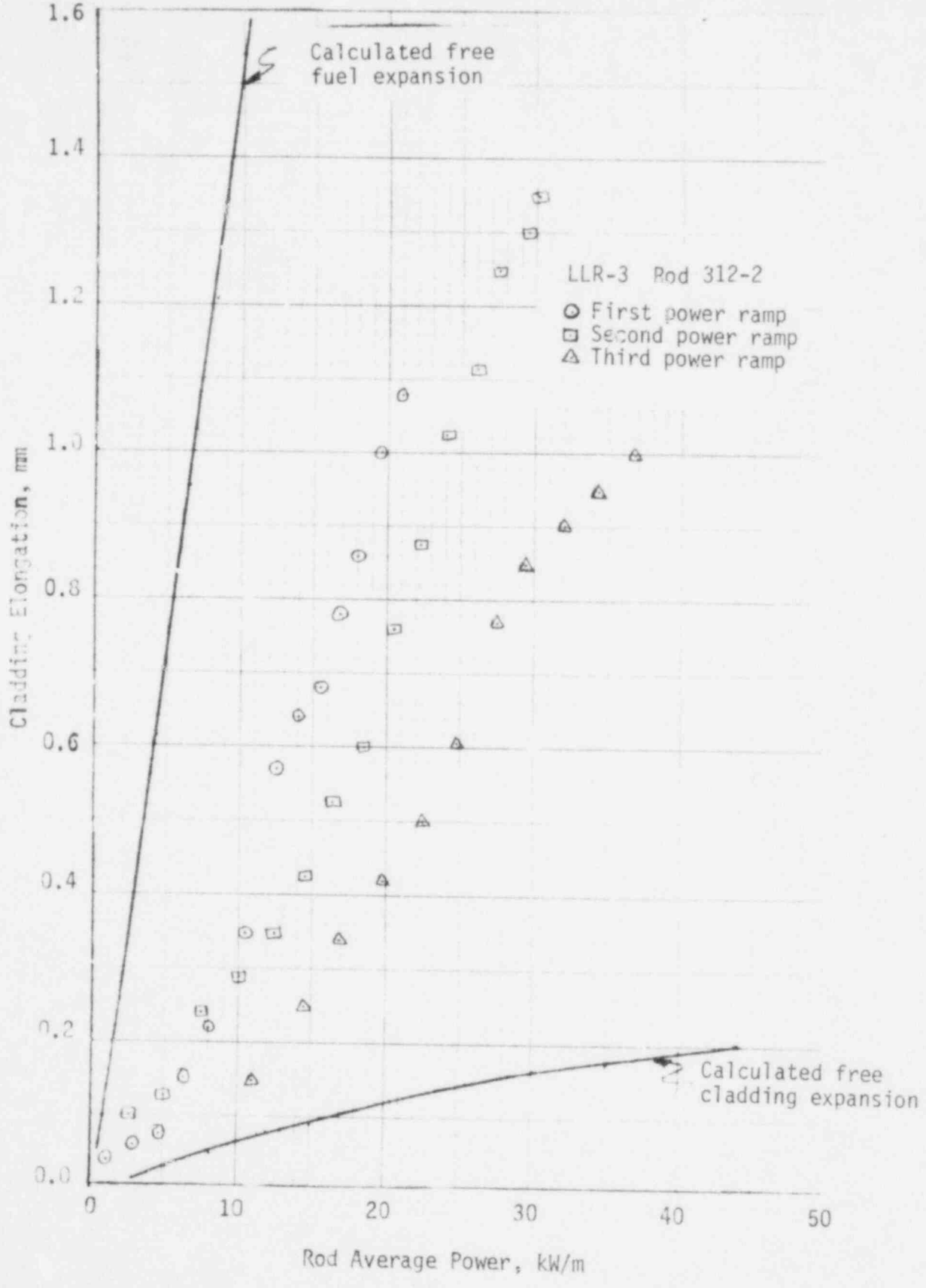


Figure 4 Fuel rod 312-2 cladding elongation versus rod average linear heat rate for the first three LLR-3 power ramps.

TABLE III

POWER RAMP RATES FOR THE PBF/LOFT LEAD ROD TEST SERIES

| Test | Ramp Number | Fuel Rod Number | Effective Ramp* Rate (kW/m-hr) | Elongation At 20 kW/m (mm) |
|---|---|---|---|---|
| LLR-3 | 1 | 312-2 | 9.9 | 1.2 |
| | 2 | 312-2 | 15.3 | 0.7 |
| | 3 | 312-2 | 17.4 | 0.4 |
| LLR-5 | NA | 345-2 | 4.8 | 0.4 |
| LLR-4 | NA | 345-2 | 3.6 | 0.1 |
| LLR-4A | NA | 345-2 | 4.7 | 0.3** |

* The average rate the fuel rod power was increased from the time the power ramp first started to the time the desired power level was reached.

** Elongation after a 1.16 mm initial permanent offset is subtracted.

LLR-3 (Table III), clearly demonstrates the ramp rate dependence. It is noted that these are both first ramp data. Cladding elongations obtained from fuel rod 345-2 during the power ramps for tests LLR-5, LLR-4, and LLR-4a are provided in Figure 5. The elongation data obtained during the power ramp for test LLR-4 represents the second ramp for rod 345-2 and when compared with data from the previous ramp, the dependence of the elongation on the number of ramps is again observed. The LLR-4 data, however, is very close to the elongation calculated for the free thermal expansion of the cladding, which may indicate that little reduction in the elongation would be observed on any future power ramps. The elongation for the next power ramp, i.e., the power ramp for test LLR-4a is also included in Figure 5. These data show, however, two significant differences from the elongation observed during the previous LLR-4 power ramp. First, the elongation for the LLR-4a test has an approximate 1.2 mm initial offset and, second, the slope of the elongation versus power level is larger for the LLR-4a test. Both differences may be the result of cladding collapse that occured during the blowdown phase for test LLR-4. Cladding collapse occurs at a time during blowdown when the cladding is at an elevated temperature and the external pressure is still sufficiently large to cause plastic deformation. If, after collapse, the cladding is rapidly cooled, e.g., quenched by reflood, the cladding would shrink onto the fuel and result in sufficient PCI to hold the cladding in a state of permanent elongation. As the fuel rod was subsequently ramped to power, the fuel would thermally expand more than the cladding, increasing the PCI and resulting in greater elongation than observed on the previous ramp. It appears, therefore, that the data in Figure 5 do show a relationship between cladding deformation and elongation. It is noted however, that the data for the LLR-4a test in Figure 5 are based on the power for rod 345-1 rather than rod 345-2. (Power data for rod 345-2 were not available.) It is doubtful that differences in the rod power would significantly change the character of the data.

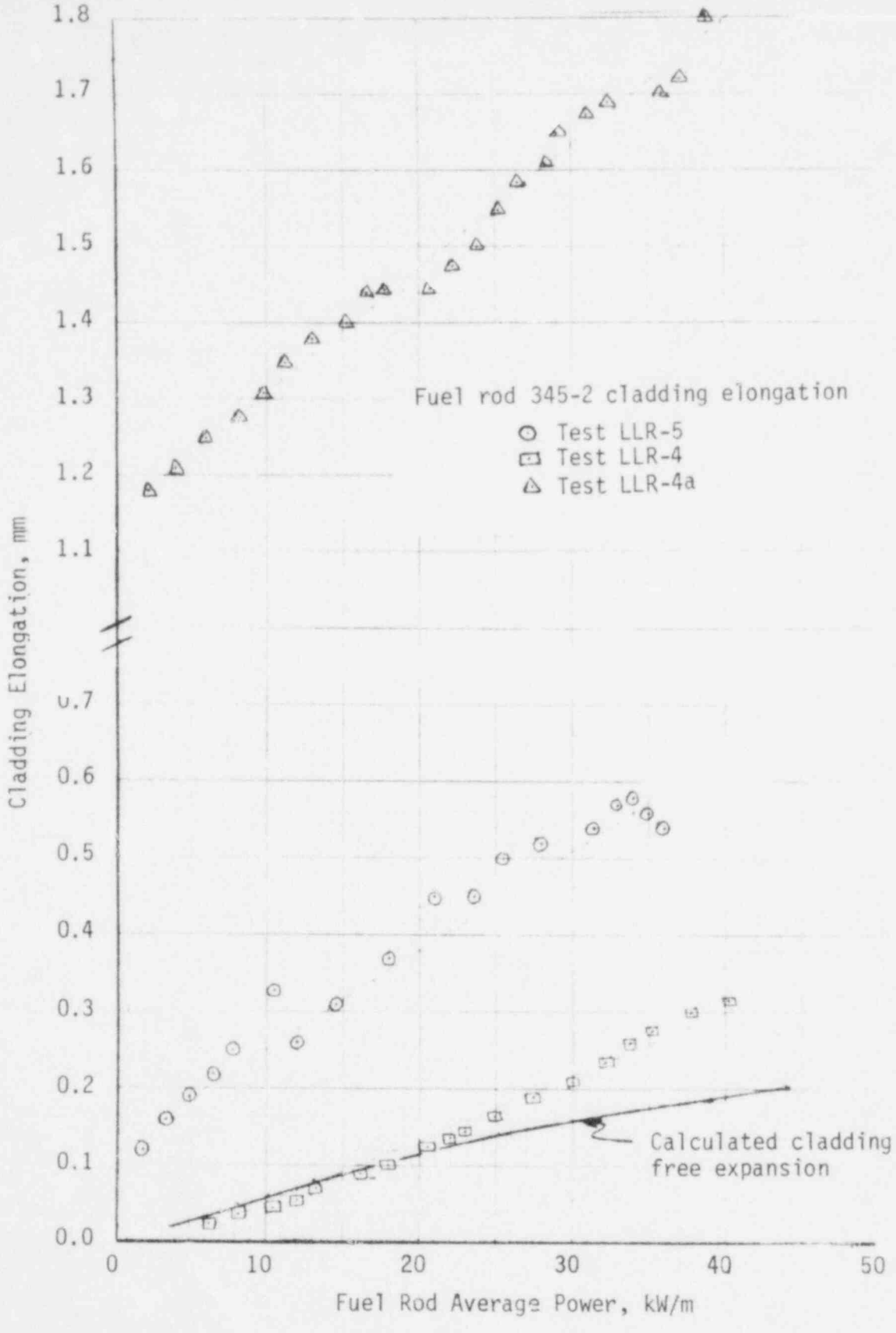


Figure 5 Fuel rod 345-2 cladding elongation versus rod average linear heat rate for the LLR-5, LLR-4, and LLR-4a power ramps.

There were significant differences in the elongation data between fuel rods for the same test. For example, the elongation data from fuel rod 312-1 for the LLR-5 and LLR-4 power ramps, which are shown in Figure 6, were considerably greater than the corresponding data for rod 345-2, shown in Figure 5. Not only is the elongation for rod 312-1 greater but rod 312-1 had experienced several additional power ramps, during the LLR-3 test, which rod 345-2 had not. Because of the effect of the number of power ramps, the difference in elongation between these rods is probably greater than appears by comparing the data in Figures 5 and 6. Based on these data, the elongation response can be different for each fuel rod. A possible explanation is that the PCI causing the cladding elongation is occurring at a different axial location for each rod. Consequently the observed elongation reflects the thermal expansion of two different fuel stack lengths.

The following observations were made from the analysis of the LLR cladding elongation data:

(1) Cladding elongation data are complicated by the effects of the number of power ramps and the ramp rate.

(2) The cladding elongation response of one fuel rod can be significantly different from that of another.

(3) The elongation data in Figure 5 indicate that it is possible to detect cladding collapse from the elongation data.

Based on these observations, it is concluded that cladding collapse and waisting that may occur during a LOCE can probably be detected by the cladding elongation data obtained during subsequent power ramps. To assure that the data being observed is the result of cladding collapse will require careful and continuous monitoring of the elongation data. This conclusion is based on data from a single rod and a single test and

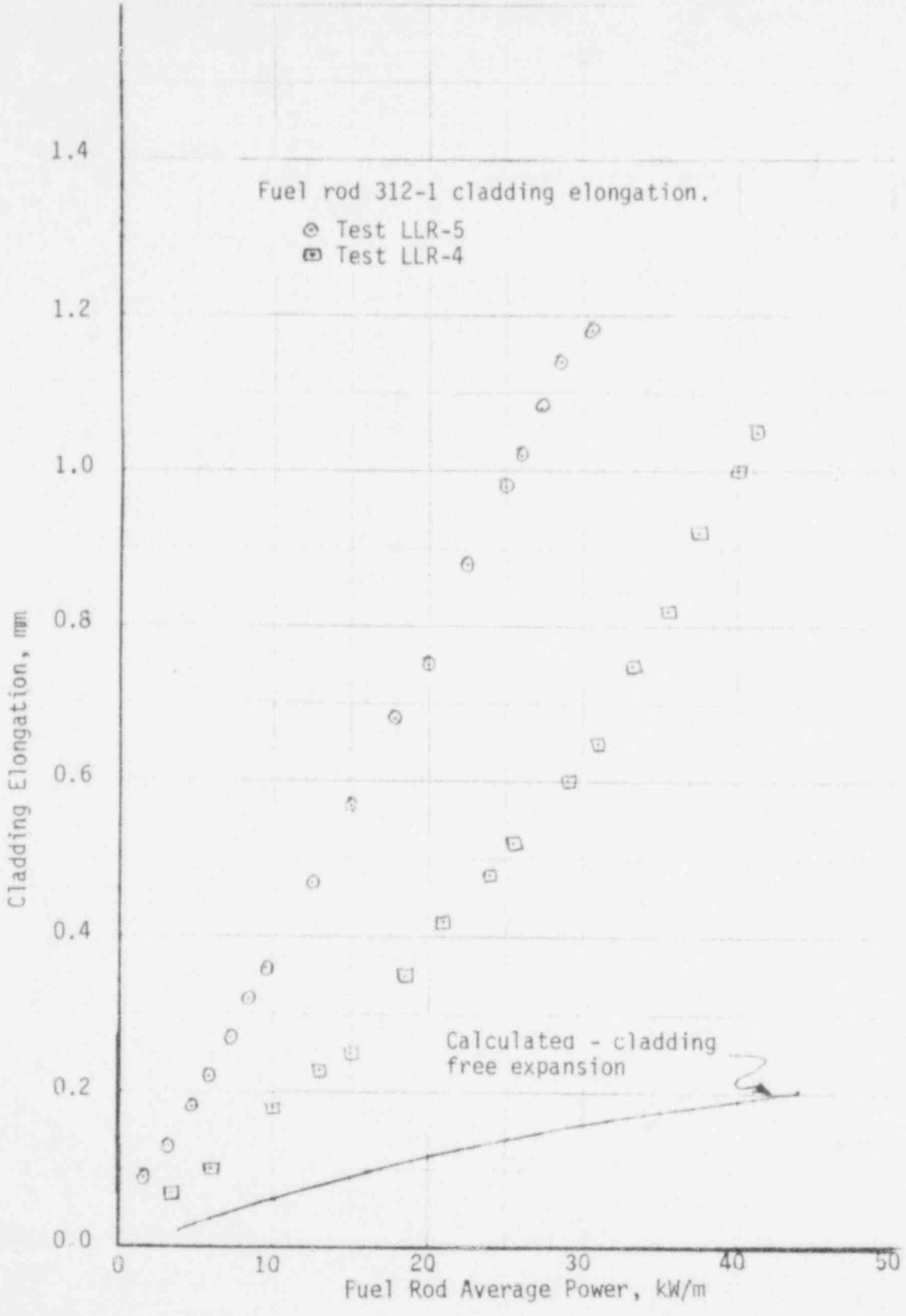


Figure 6 Fuel rod 312-1 cladding elongation versus rod average linear heat rate for the LLR-5 and LLR-4 tests.

confirmation of a correlation between cladding elongation and collapse will require the review of additional data and perhaps a better understanding of the relationship between cladding elongation and the number of ramps and ramp rate.

## 4.2 Fuel Centerline Temperature

The objective of analyzing the fuel centerline temperatures under steady-state conditions was two-fold; (a) to determine if cladding deformation could be detected by monitoring the centerline temperature and (b) to evaluate the capability of FRAP-T5 to accurately predict centerline temperatures for LOFT type fuel with and without collapsed cladding. Analysis of centerline temperatures presented here compares data obtained from the quasi-steady state power ramps with calculations that considered steady-state conditions. In doing this, it was assumed that ramp rates $\leq$4.8 kW/m-hr represented steady-state conditions.

The temperature data considered for this analysis were taken from rods 345-1, 345-2, and 399-2 during tests LLR-5, LLR-4 and LLR-4a. These data are shown in Figures 7, 8, and 9 for the respective rods. Centerline temperature data from fuel rods 312-1, 312-2, 312-3 and 312-4 were not considered for this analysis. The data from these rods were given a qualification type 2 (trend only) as indicated by Table II. Centerline thermocouples (TC's) for rods 312-1 and 312-2 were not properly installed (refer to Section 5.1). The TC for rod 312-3 had failed and the TC for rod 312-4 indicated intermittent failure.

The calculated centerline temperature data in Figures 7, 8 and 9 for a fresh, uniradiated fuel were based on the nominal, BOL fuel rod dimensions given in Table I and the coolant conditions measured during the steady-state or fuel preconditioning phase for the LLR-5 test. Although the calculation is based on coolant conditions from test LLR-5, the calculated centerline temperature data are applicable to any test involving

fresh fuel since inlet coolant conditions during the preconditioning phases were essentially the same for all tests. The calculated centerline temperature data in Figures 7 and 8 for collapsed cladding were obtained from a FRAP-T5 calculation initialized from the end-of-test conditions calculated for LLR-4 since the cladding was predicted to collapse during this test.

The centerline temperature data obtained from fuel rod 345-1 during the power ramping phase of tests LLR-5, LLR-4 and LLR-4a are shown in Figure 7. At linear heat rates up to 30 kW/m, the data from tests LLR-5 and LLR-4 are in good agreement. For linear heat rates greater than 30 kW/m, however, the data start to diverge with the temperature data from the LLR-4 test being less. Although the smaller temperatures for LLR-4 could be attributed to cladding deformation during the LLR-5 test, the transient analysis for LLR-5 (refer to Section 5.1.2) indicate cladding collapse did not occur at the location of the cladding thermocouples. Also, the data from fuel rod 345-2 during the same power ramps (refer to Figure 8) do not show the same relative behavior. The larger centerline temperatures observed at power levels greater than 30 kW/m during the LLR-5 power ramp may have been the result of significant pellet relocation causing an increase in the rod thermal resistance.

In comparing the centerline temperature data obtained from rod 345-1 (Figure 7), the data for LLR-4a is noted to be consistently lower than the data obtained on the previous power ramps. Reduced centerline temperatures are indicative of a larger gap conductance, which would result from collapsed cladding. These temperature data, therefore, indicate cladding collapse and support the conclusion made in the transient analysis for rod 345-1 (refer to Section 5.1.3) that the cladding collapsed at the location of the thermocouples for rod 345-1 during the blowdown phase of test LLR-4. In addition rod 312-1, removed after LLR-4 for postirradiation examination, showed collapse and waisting and comparable deformation would be expected on other fuel rods.

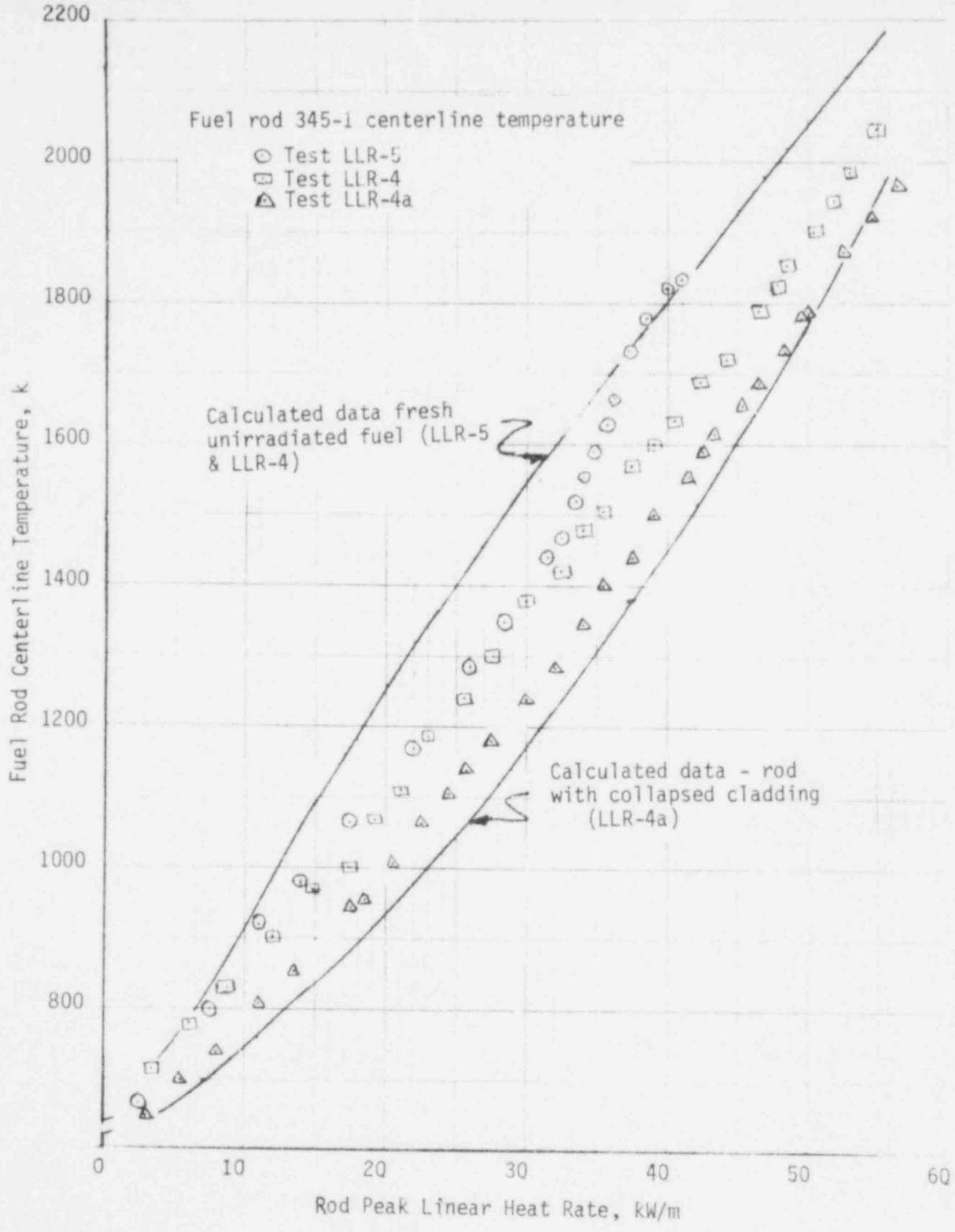


Figure 7 Calculated and measured centerline temperature versus rod peak linear heat rate. Measured data from fuel rod 345-1, tests LLR-5, LLR-4, and LLR-4a.

The centerline temperature data obtained from rod 345-2 during the power ramp phase of tests LLR-5 and LLR-4 are shown in Figure 8. In general, these data are somewhat lower than the corresponding data for rod 345-1. Centerline temperature data obtained from rod 345-2 during the LLR-4a power ramp are not included in Figure 8 because rod power data were not available for this rod during the LLR-4a power ramp since instrumentation measuring the differential coolant temperature had failed.

The centerline temperature data obtained from rod 399-2 during the LLR-4a power ramp is shown in Figure 9. Fuel rod 399-2 was a fresh, unirradiated fuel rod for this test and consequently the data should be compared to the calculated data for a fresh unirradiated fuel rod. These data are consistently larger than the centerline temperature data for fuel rods 345-1 and 345-2. They are, however, in better agreement with the calculated data for power levels up to 30 kW/m. At power levels above 30 kW/m, the calculated temperatures are less than the measured data.

From the analysis of the steady-state centerline temperature data and comparison of calculated with measured data, the following observations are made:

(1) In general, FRAP-T5 over predicts the steady-state centerline temperatures for LOFT type fuel without collapsed cladding.

(2) In general, FRAP-T5 underpredicts the centerline temperatures for fuel rods with collapsed cladding.

(3) A significant difference occurs in the measured centerline temperature (up to 100 K) for fuel rod 345-1 with and without collapsed cladding.

(4) Significant differences occur in the measured centerline temperature for identical fresh unirradiated fuel.

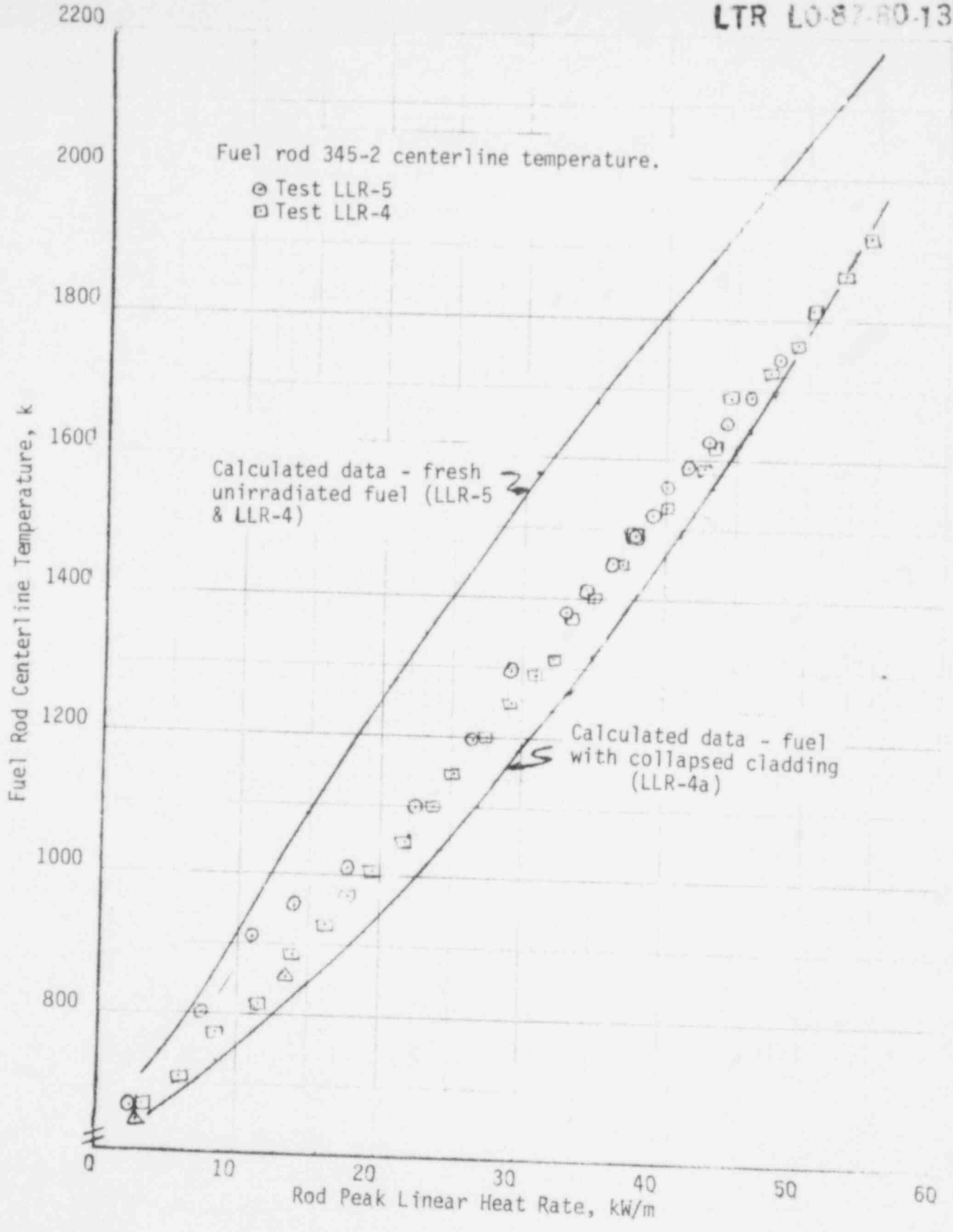


Figure 8 Calculated and measured centerline temperature versus rod peak linear heat rate. Measured data from fuel rod 345-2, tests LLR-5 and LLR-4.

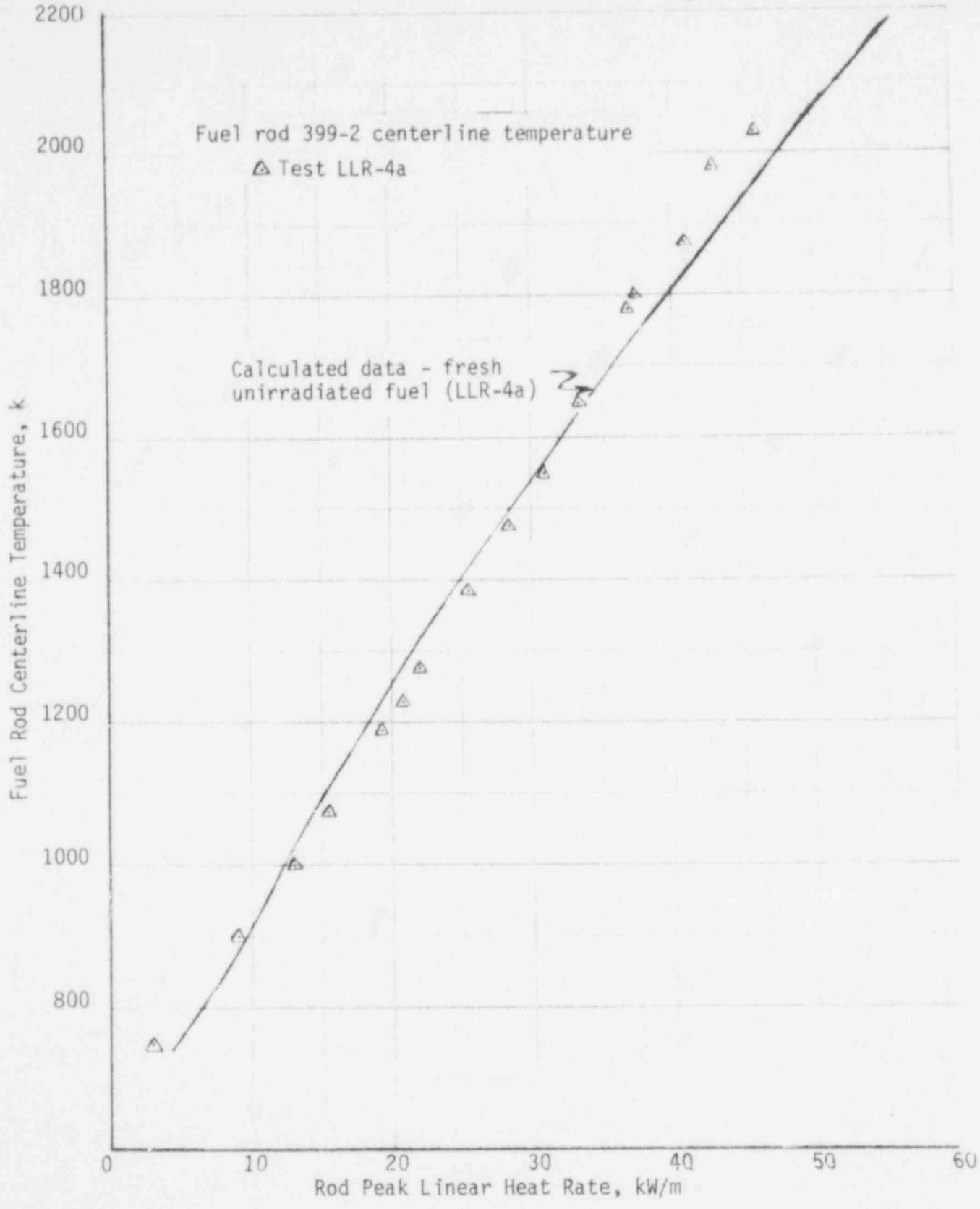


Figure 9 Calculated and measured centerline temperature versus rod peak linear heat rate. Measured data from fuel rod 399-2, test LLR-4a.

Based on the last two observations, it is concluded that cladding collapse occurring during a LOCE can be detected from centerline temperature data, however, a continuous monitoring of the centerline temperature will be required on individual rods. This conclusion is based on data from a single fuel rod and from a single test and consequently confirmation of a correlation between cladding deformation and centerline temperature will require the review of additional data.

# 5. TRANSIENT ANALYSIS

The primary purpose for the transient analysis was to evaluate the possibility of using the FRAP-T5 computer code as a tool for assessing the condition of the LOFT fuel after a LOCE and as a tool for requalifying the LOFT core for additional tests. In this regard, the capability of FRAP-T5 to accurately predict cladding collapse was evaluated. This evaluation was accomplished by comparing calculated transient centerline temperature with the data.

In addition to the primary purpose, the centerline temperature data from rods with and without cladding surface TC's were reviewed and compared in an effort to identify possible enhanced cooling attributable to the surface TCs.

## 5.1 Capability of FRAP-T5 to Predict Cladding Collapse

In support of the FRAP-T5 evaluation, all transient calculations were performed by requiring the calculated cladding surface temperature to be equal to the measured cladding temperature as discussed in Section 3. The coolant pressure measured during the blowdown was also input in order to realistically calculate cladding collapse.

For fresh, unirradiated fuel, the calculation was based on the nominal, beginning-of-life (BOL) fuel rod data given in Table I. When the calculation considered a fuel rod that had been in a previous LOCE, the calculation was initiated from the end-of-test conditions calculated for the previous test. Whether a calculation was initialized from BOL input or calculated end-of-test conditions will be indicated in the discussion for each calculation.

The cladding temperature measurements were limited to one or two closely spaced (7.6 cm) axial locations. Consequently, the axial temperature distribution during blowdown and reflood were not measured. No attempt was made to calculate the axial fuel rod elongation during the transient since the FRAP-T5 calculations were single node calculations, which calculated the thermal and mechanical behavior for the region represented by the cladding temperature measurements. (A review of the LVDT transient data is presented in Reference 8).

5.1.1 LLR-3 Rod 312-2. The measured cladding surface and fuel centerline temperatures are compared with the calculated fuel centerline temperature for fuel rod 312-2 at the 0.457 m elevation during the LLR-3 test in Figure 10. After the initiation of blowdown, the centerline temperature starts to decline almost immediately. This is as would be expected since the reactor was scramed at the time blowdown was initiated, which would immediately reduce the power being generated in the fuel rod. From 10 to 25 s into the transient, however, the test data indicate a gradual increase in the centerline temperature from 1090 to 1200 K. At approximately 25 s, the temperature levels off and remains essentially constant until the test is terminated by reflood at 37 s. At ten seconds, the cladding surface temperature, also shown in Figure 10, is essentially constant at 905 K; indicating the fuel rod is in a stable film boiling with radiation heat transfer. If the power level at this time were large enough to cause an increase in the fuel temperature, a similar increase in the cladding temperature would also be expected.

The temperature data obtained from the centerline thermocouples in rods 312-1 and 312-2 (data in Figure 10) have been categorized as trend information for all LLR tests involving these two fuel rods. The design of thermocouples (tungsten, 5% rhenium vs. tungsten, 26% rhenium) for the measuring of centerline temperatures for the LLR test series used compensating wire for the major portion of the instrument leads. In this design, the junctions of the thermocouple and compensating wire are made at

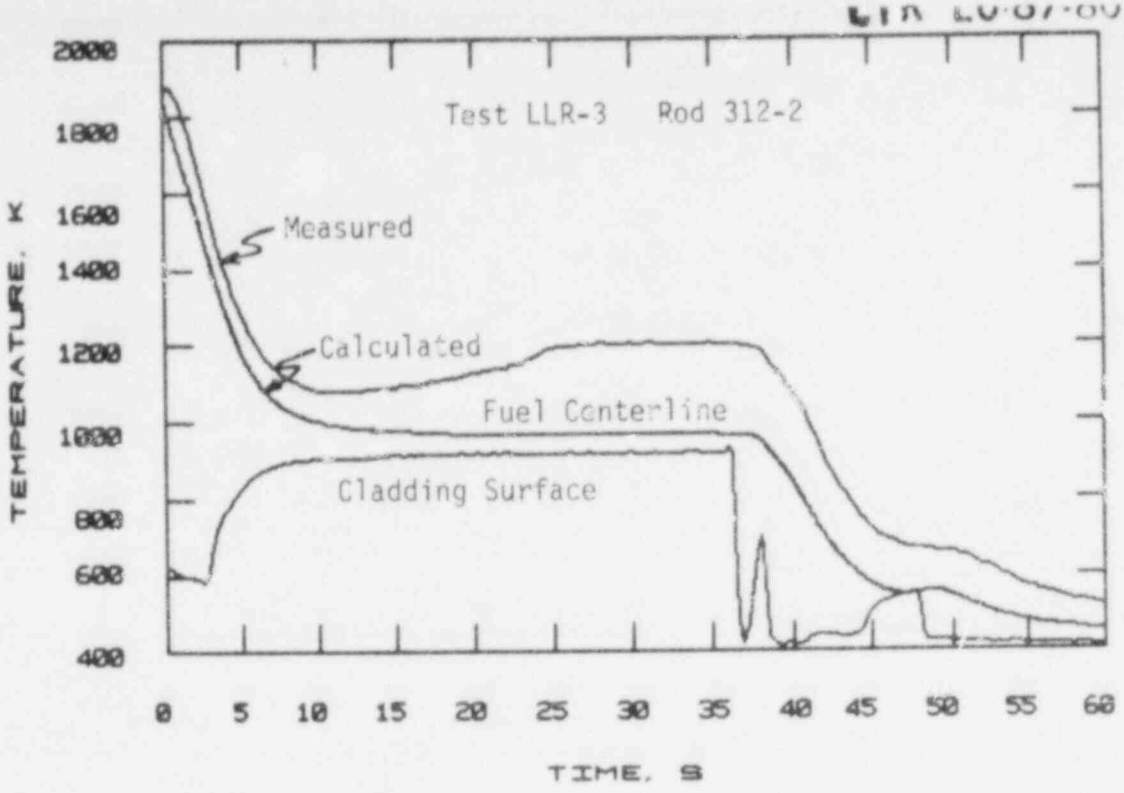


Figure 10 Calculated and measured centerline temperature with an overlay of the measured cladding surface temperature. Fuel rod 312-2, test LLR-3.

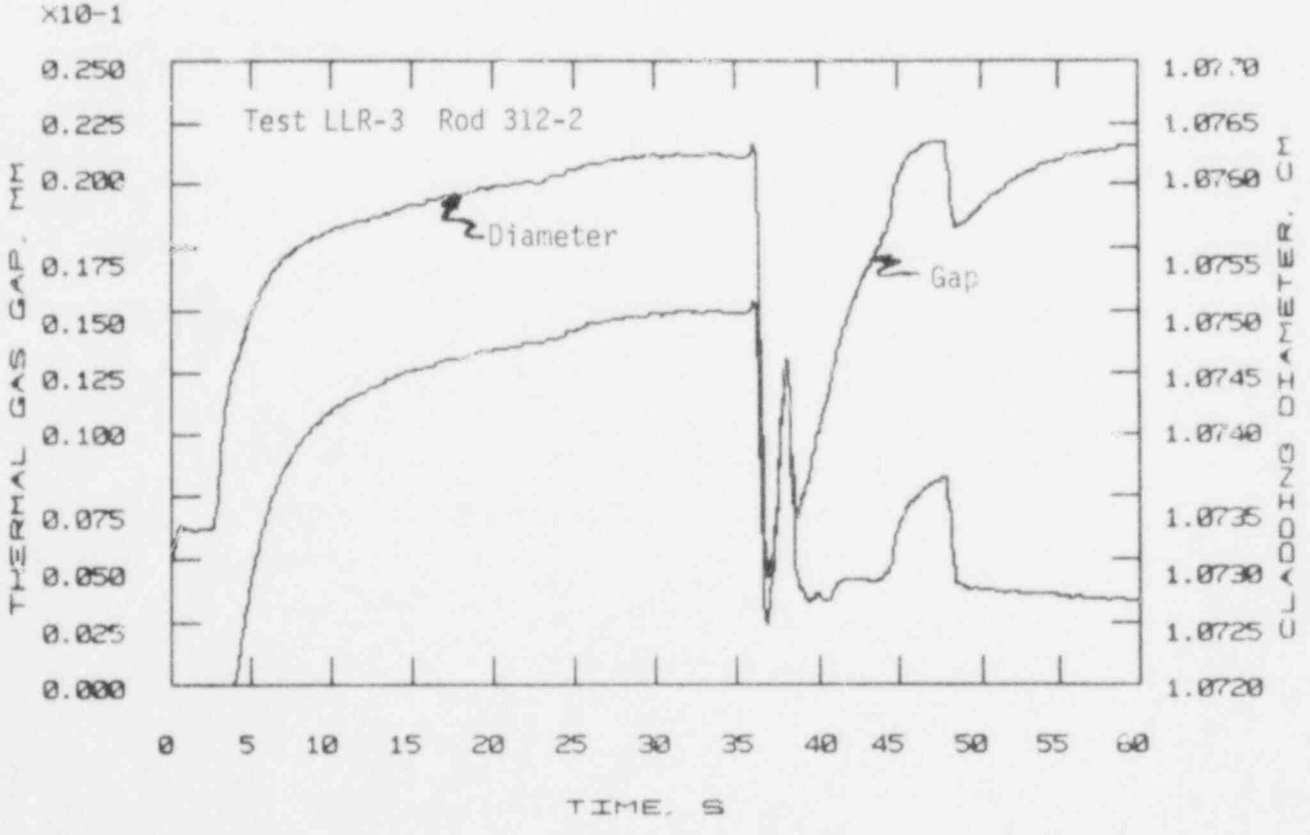


Figure 11 Calculated thermal gas gap and cladding OD corresponding to the data in Figure 10.

a location of lower temperature and in this case, the junctions were located in the fuel rod upper plenum. During the fabrication process the compensating wires were inadvertently connected to the wrong thermocouple wires, which resulted in a reversed polarity between thermocouple and the compensating leads. As a result, it was necessary to apply correcting factors to the recorded data and consequently the data have been categorized as trend information. The measured data in Figure 10 is the corrected data.

Based on these observations it is concluded that the centerline temperature data, from fuel rods 312-1 and 312-2, are not suitable for evaluating the FRAP-T5 code and consequently the transient analyses for the LLR tests utilized rod 345-1 for subsequent tests. No attempt was made to calculate the response of the other fuel rods (rods 312-3 and 312-4) in the LLR-3 test. Either the centerline thermocouples failed or demonstrated intermittent failure for rods 312-3 and 312-4 during this test.

FRAP-T5 predicted no cladding deformation or permanent hoop strain for rod 312-2 during the LLR-3 test. The outside cladding diameter and the corresponding thermal gas gap calculated by FRAP-T5 for the LLR-3 test is shown in Figure 11. The thermal gap is based on the Coleman relocated pellet correlation[3] which assumes that pellet cracking and relocation occurs at low powers. Although FRAP-T5 calculates the thermal gap to be initially closed and to remain closed for the first four seconds of the LLR-3 blowdown, the code calculates no interfacial pressure. Thus, a closed thermal gap does not necessarily mean interfacial pressure or hard pellet-cladding contact.

5.1.2 LLR-5 (Rod 345-1). Rod 345-1 was a fresh unirradiated fuel rod in test LLR-5; having replaced rod 312-3 which failed in test LLR-3. Rod 345-1 was chosen for the continuation of the LLR posttest analysis since it was included for the remainder of the test series and had cladding surface thermocouples necessary for input to the calculations. Rod 345-2,

which replaced rod 312-4 after LLR-3, did not have surface thermocouples. Since rod 345-1 was a fresh fuel rod in the LLR-5 test, the FRAP-T5 calculation was initiated from the data in Table I. The calculated and measured centerline temperature data for the LLR-5 test, rod 345-1, are illustrated in Figure 12. The measured cladding surface temperature is also included in the figure for reference. The surface thermocouple was located at 0° azimuthal (refer to Figure 1) and was approximately 7.6 cm above the midplane of the active fuel column.

Reactor scram for the LLR-5 test was delayed approximately two seconds after initiation of blowdown. Prior to blowdown, the steady-state centerline temperature was 1825 K. After blowdown was initiated, the temperature shows a slow decline for the first two seconds, which is indicative of the delayed scram and the continuation of normal heat transfer. At approximately two seconds, the temperature begins a rapid descent in response to the rapidly decaying power and two rewets[a] that occur after the initial critical heat flux (CHF). These rewets are reflected in the cladding surface temperature data included on Figure 12. Although stable film boiling is established by five seconds, the centerline temperature continues its rapid descent as the energy in the center portions of the fuel pellet is redistributed to the cladding and the surface region of the pellet. By 15 s the enthalpy redistribution is nearly complete and the centerline temperature begins a slow decline indicative of film boiling and radiation heat transfer to the cooler shroud.

The FRAP-T5 calculation for test LLR-5, rod 345-1 was initiated from input describing a nominal BOL fuel rod (refer to Table I) and the cladding surface temperature measured at the 0° azmuthal location[b].

---

a. Rewet refers to cooling transients that occur shortly after CHF that reducing the cladding temperature before it has reached a maximum and are attributed to a leaky check valve.

b. This fuel rod had two thermocouples on the cladding surface at 0.533 m elevation; one at the 0° and the other at 180° azimuthal location. Refer to Figure 1.

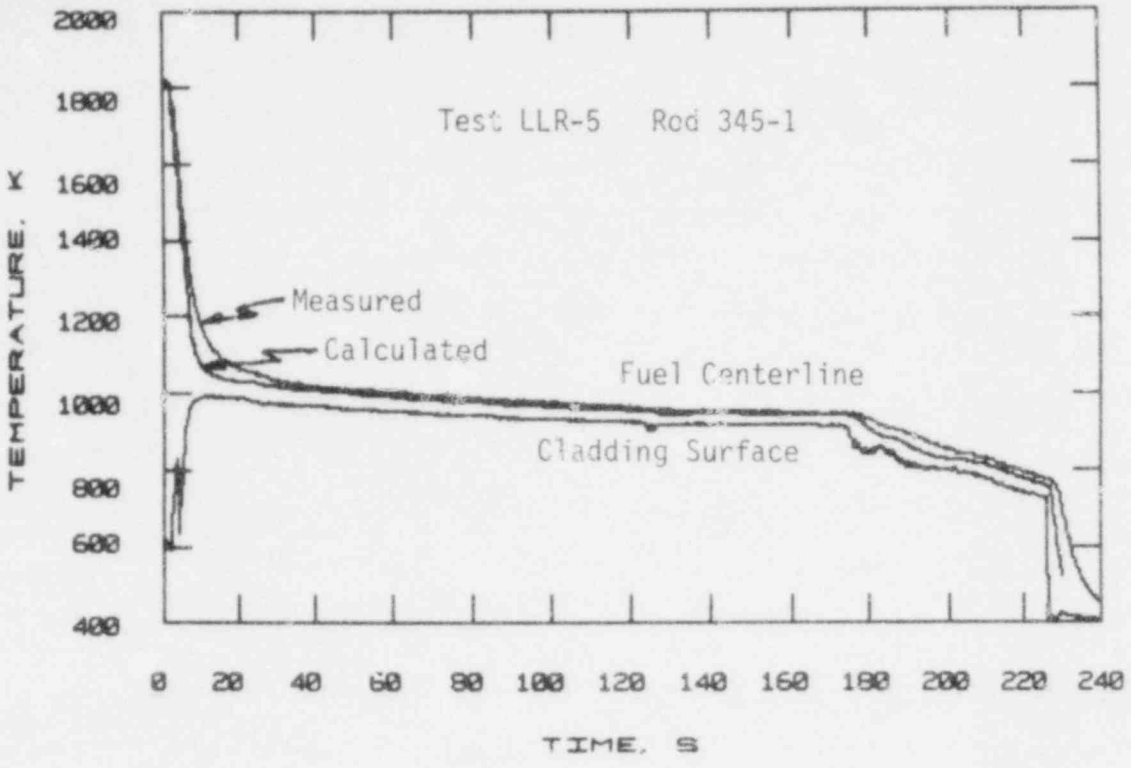


Figure 12 Calculated and measured centerline temperature with an overlay of the measured cladding surface temperature. Fuel rod 345-1, test LLR-5. Cladding collapse calculated.

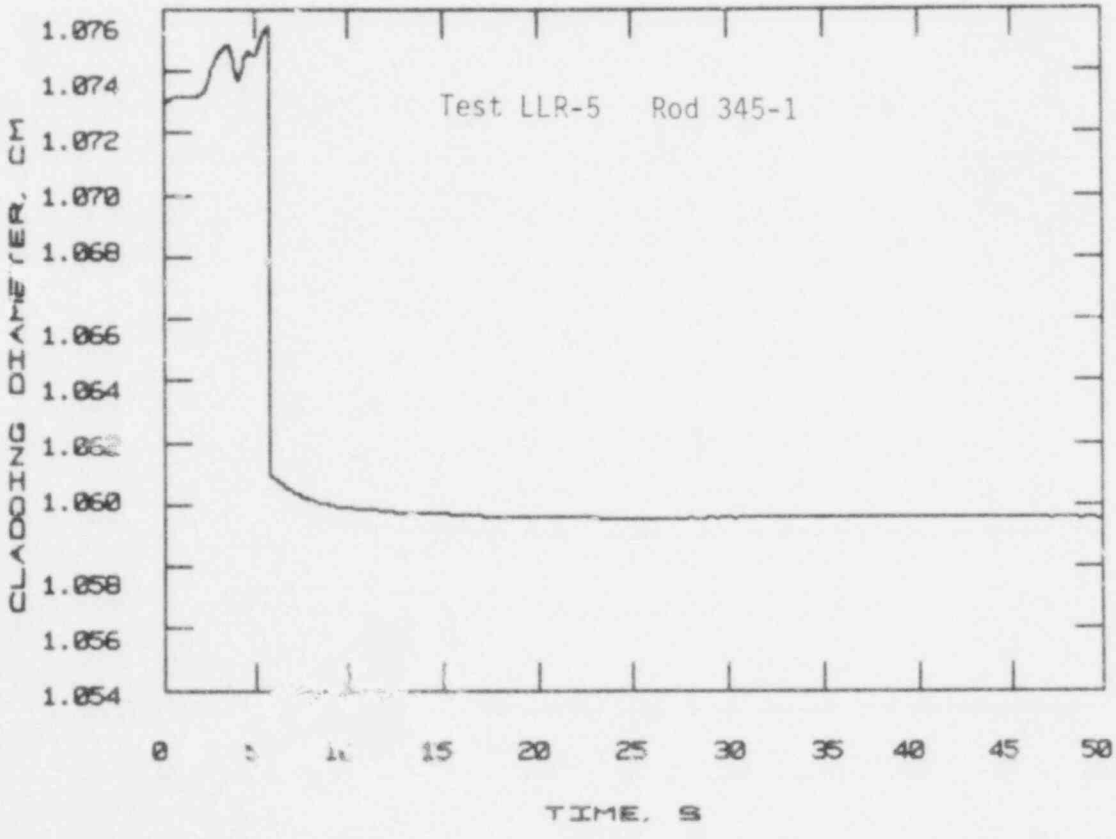


Figure 13 Calculated cladding OD corresponding to data in Figure 12.

In addition to the fuel rod parameters and the measured cladding temperature, input to the calculation included the coolant pressure measured during the blowdown phase of the test. By comparing the measured and calculated centerline temperature data in Figure 12, it can be seen that the data are in good ag eement except for the 6 to 35 s interval where the calculated data are up to 105 K lower than the measured. Upon reviewing the calculated data, it was noted that FRAP-T predicted cladding collapse to occur and as seen by the calculated cladding diameter in Figure 13, this was predicted to occur at about six seconds.

Based on tne data in Figure 14, which compares the measured cladding temperature and ambient rod pressure with C. S. Olsen's cladding deformation data[10], uniform cladding collapse would not have occurred. Olsen investigated fuel rod cladding deformation in isothermal, isobaric conditions for zircaloy cladding. These out-of-pile tests provide data to defined the pressure-temperature thresholds, shown on Figure 14, for three degrees of deformation; (a) buckling, (b) collapse, and (c) waisting. Buckling being defined as a severe cladding ovality that results in two point pellet-cladding contact. Collapse refers to a uniform circumferential collapse onto the fuel pellets and waisting refers to a plastic flow of the cladding into the small axial gaps between pellets. The data in Figure 14 indicate that buckling probably occurred at the location of the tnermocouples during test LLR-5 but it is unlikely that the cladding actually collapsed uniformly onto the fuel.

The thermal gas gap calculated by FRAP-T5 is initially closed and remains closed throughout the transient. At the time of cladding collapse, the calculated pellet-to-cladding interfacial pressure increases to 12.8 MPa and the calculated gap conductance increases from 24.7 to 61.4 $kW/m^2$ K. Although the interfacial pressure drops to 4.0 MPa within two seconds after collapse, the gap conductance remains at 61.4 $kW/m^2$-K for 14 s. At this time (20 s transient time) the pressure has declined to 0.95 MPa and returns to zero at 25 s. Refering again to Figure 12, it is

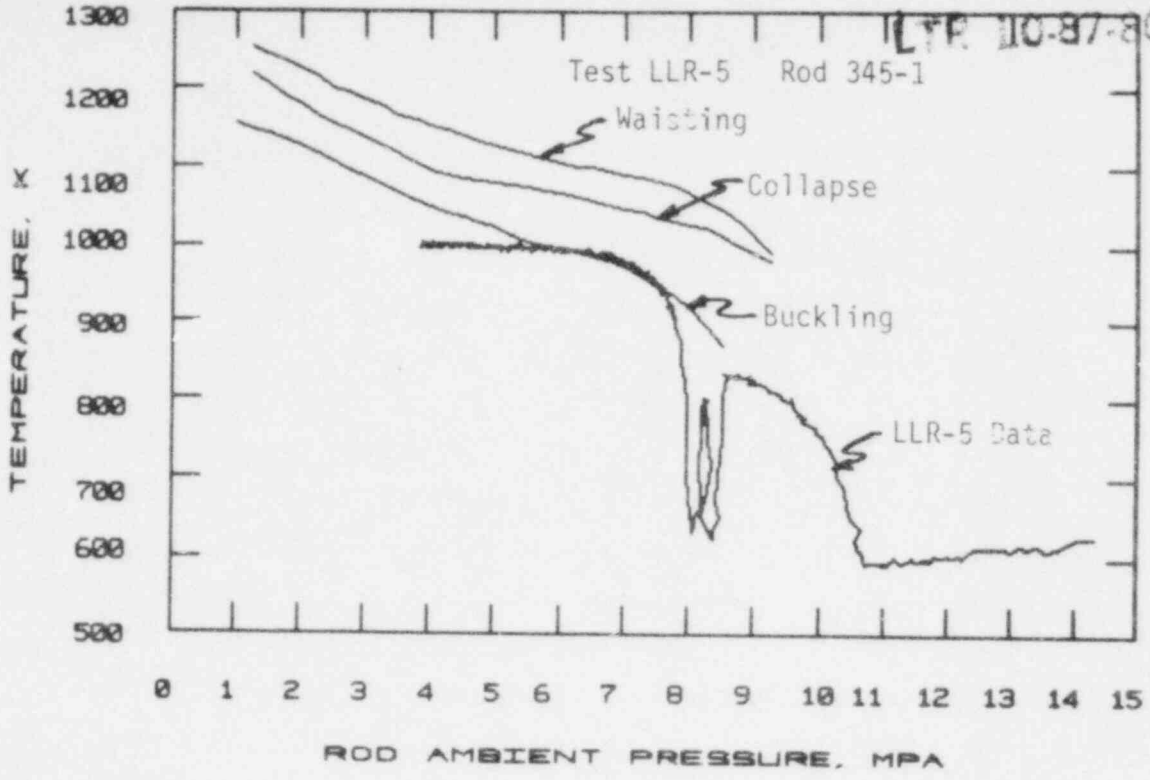


Figure 14 A comparison of measured cladding temperature and external pressure with cladding deformation data. Rod 345-1, test LLR-5.

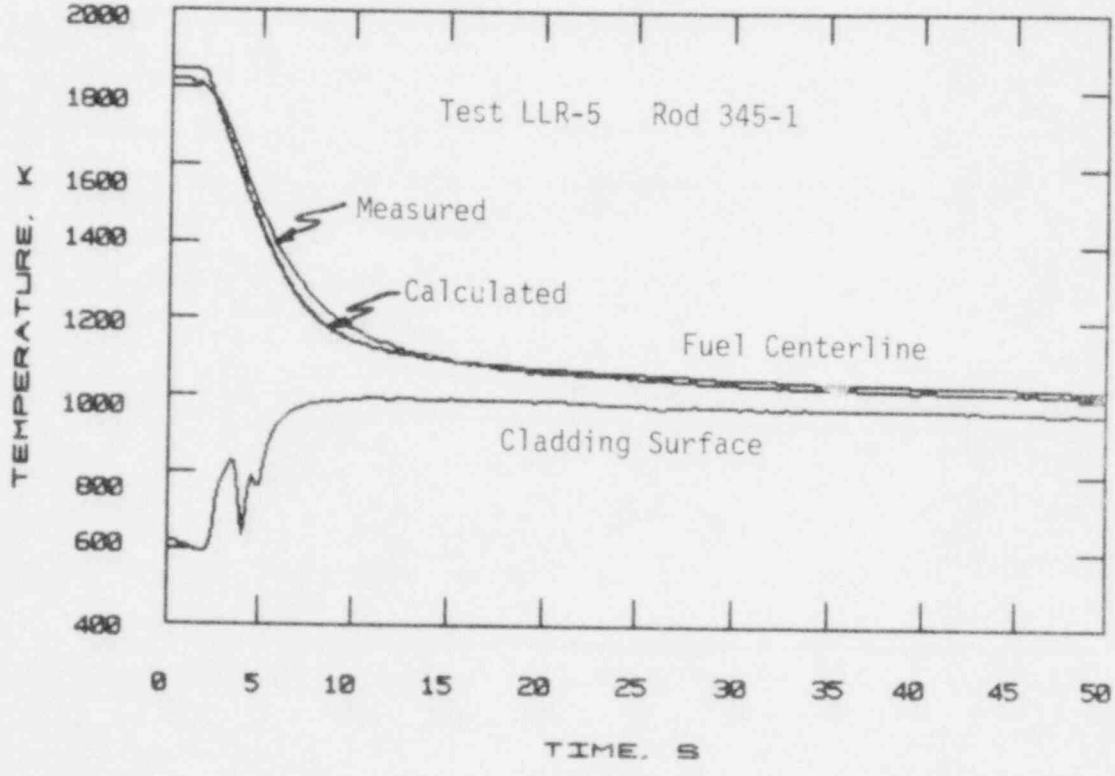


Figure 15 Calculated and measured centerline temperature with an overlay of the measured cladding surface temperature. Fuel rod 345-1, test LLR-5. No cladding collapse calculated.

noted that the interval of predicted interfacial pressure (6 to 25 s) and a corresponding large gap conductance, is essentially the same time interval of significant differences between calculated and measured centerline temperatures. Furthermore, if cladding collapse did not occur, as substantiated by Olsen's data in Figure 14, the calculated gap conductance would be less during the 6 to 25 s interval and consequently the calculated and measured fuel centerline temperature would be in better agreement. To check this hypothesis, the coolant pressure input to FRAP-T5 was arbitrarily reduced to assure no cladding collapse and the calculation redone. The centerline temperature response calculated for this case is presented in Figure 15 with the measured response. These data show the calculated and measured centerline temperatures compare much better; within 40 K for the duration of the calculation.

The cladding diameter and corresponding thermal gap calculated by FRAP-T5 (for the no-collapse case) are shown in Figure 16. As in the previous calculation, the thermal gas gap is initially closed but it is now predicted to open at approximately five seconds; shortly after established film boiling and the cladding begins to thermally expand. It is noted that the initial cladding diameter in Figure 16 is slightly greater ( 0.01 mm) than the initial diameter in Figure 13. The difference is not the result of permanent cladding strain (both calculations started with fresh unirradiated fuel) but elastic strain caused by the difference in coolant pressure. Apparently this small increase in diameter results in a decrease in the gap conductance and a corresponding increase in the initial centerline temperature; 1815 K (Figure 12) to 1845 K (Figure 15). Both, however, are in good agreement with the 1825 K that was measured.

By comparing the FRAP-T5 calculation of the LLR-5 blowdown transient with the actual test data, it was determined that the code will, under certain circumstances, predict cladding collapse for LOFT type (unpressurized) fuel when collapse did not occur. In addition, a comparison of calculated and measured centerline temperatures for the LLR-5 test, indicates that FRAP-T5 calculates centerline temperatures during a

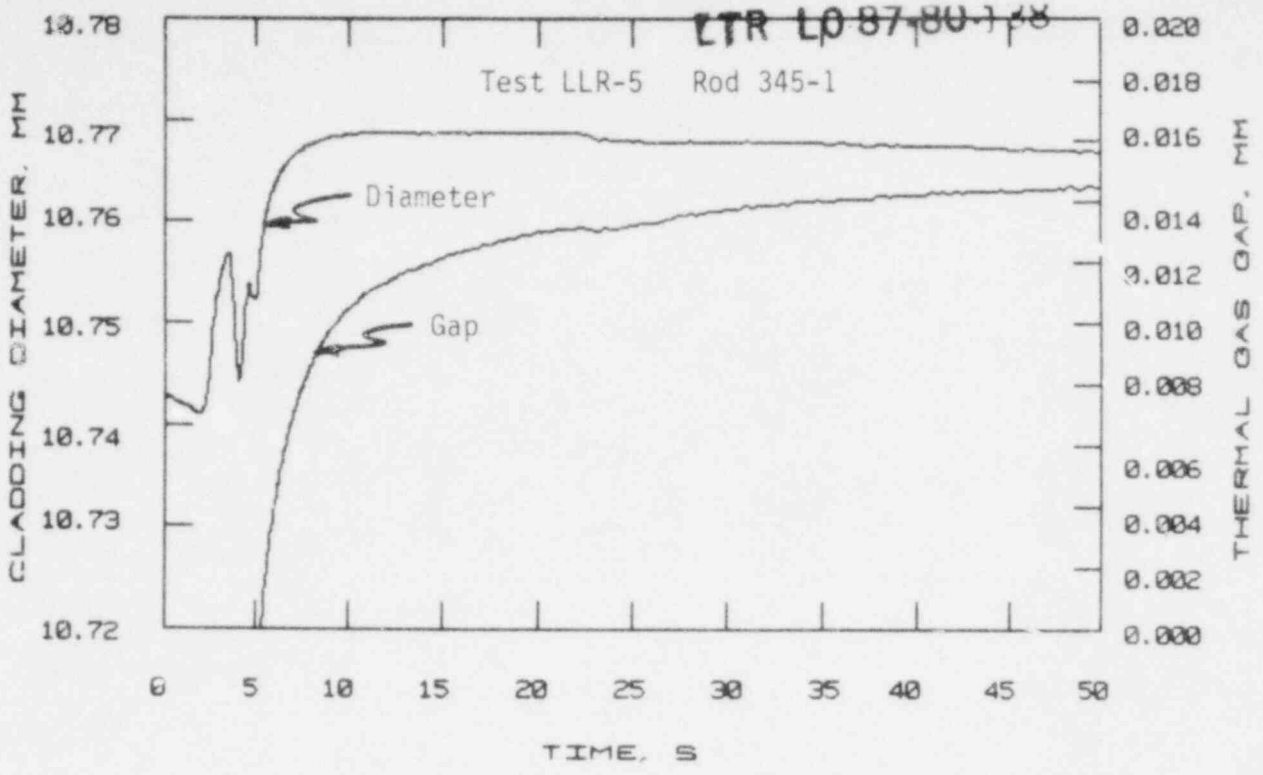


Figure 16 Calculated thermal gas gap and cladding OD corrresponding to data in Figure 15.

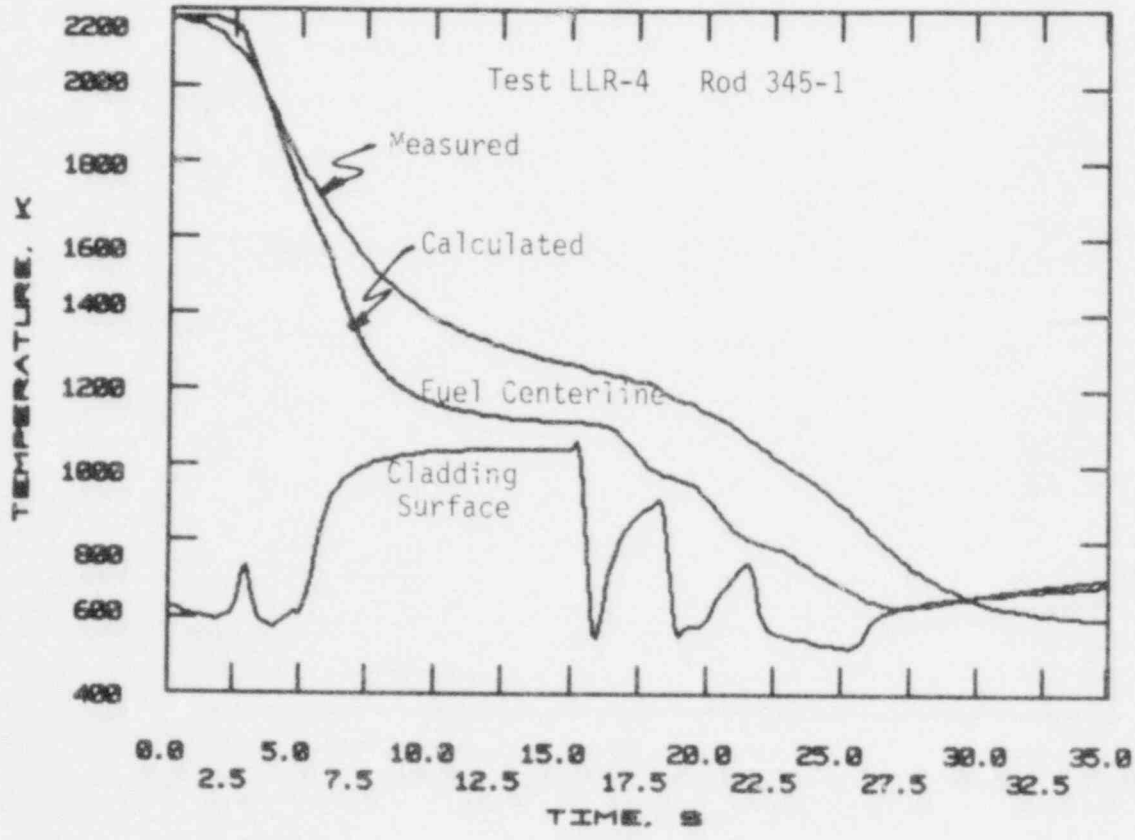


Figure 17 Calculated and measured centerline temperature with an overlay of the measured cladding surface temperature. Fuel rod 345-1, test LLR-4.

LOCE that are in good agreement with the data; at least when collapsed cladding does not exist.

5.1.3 LLR-4 (Rod 345-1). The measured cladding surface and fuel centerline temperatures are compared to the calculated centerline temperatures, for rod 345-1 during the LLR-4 test in Figure 17. Reactor scram for this test was delayed approximately 2.6 seconds after initiation of blowdown. During the steady-state operation prior to blowdown, the centerline temperature was measured to be 2190 K compared to a calculated value of 2180 K. The centerline temperature response during the first 2-3 s descends slowly until reactor scram, and then drops rapidly during the establishment of film boiling and the redistribution of the fuel enthalpy. This response was similar to the response observed early in the transient for the LLR-3 and LLR-5 tests. At about 8 s, the rate of the decrease in centerline temperature then begins to slow as film boiling continues and the redistribution of fuel enthalpy nears completion. At about 18 s, the centerline temperature again begins a rapid descent that continues for approximately 12 s. This is caused by a series of cooling transients resulting when a blowdown system isolation valve malfunctioned, allowing coolant to enter the test space. These cooling transients are observed in the cladding temperature, in Figure 17. Although by 30 s the rate of the temperature descent has reduced, it continues to drop and at 35 s it has dropped to approximately 600 K.

The FRAP-T5 calculation for test LLR-4, rod 345-1 was initiated from the end-of-test conditions calculated for the previous LLR-5 test, which resulted in no cladding collapse. The coolant pressure measured during the blowdown was input for the rod external pressure. The cladding surface temperature obtained from Rod 345-1 (0° azimuthal refer to Figure 1), shown in Figure 17 was used as the cladding temperature boundary condition.

A comparison of the calculated centerline temperature with the measured data is provided in Figure 17. At approximately six seconds

FRAP-T5 predicts the cladding to collapse onto the fuel. The cladding collapse is accompanied by a zero to 4.5 MPa increase in the pellet-to-cladding interfacial pressure and a corresponding increase in the gap conductance from 45.9 to 61.5 kW/m$^2$-K. Although the interfacial pressure declines slowly until the first coolant transient (16 s), the gap conductance remains essentially constant at 61.5 kW/m-K. At the time cladding collapse is predicted a significant increase in the divergence between calculated and measured centerline temperatures is observed to occur. This implies that FRAP-T5 is calculating a fuel rod thermal resistance that is too small for a collapsed cladding situation and/or predicting collapse before it actually occurred.

Cladding collapse is believed to have occurred on rod 345-1 during the LLR-4 blowdown. Although a comparison of the cladding temperature and ambient rod pressure data with Olsen's deformation data[10] in Figure 18 would indicate incipient collapse, post irradiation examination of rod 312-1 after test LLR-4 showed not only collapse but waisting as well. In addition, a comparison of centerline temperature data obtained from Rod 345-1 during the power ramping phases for Tests LLR-4 and LLR-4a (refer to Figure 7) indicates that the cladding had collapsed during the LLR-4 test blowdown.

The comparison of Olsen's cladding deformation data with the LLR-4 test data, which is provided in Figure 18, was used to define a region of temperature and pressure where cladding collapse was most likely to have occurred. The time interval during the LLR-4 blowdown when these conditions actually existed was then determined and defined as the estimated time of cladding collapse. This time interval is shown in Figure 19. The estimated time interval for cladding collapse was found to be 7.9 to 9.2 s, which is 2 to 3 s later than the time of collapse predicted by FRAP-T5. As seen by Figure 19, the difference between the time FRAP-T5 predicts collapse and the estimated time of actual collapse spans a large part of the time interval when the calculated and measured centerline temperatures are diverging. It is concluded, therefore, that

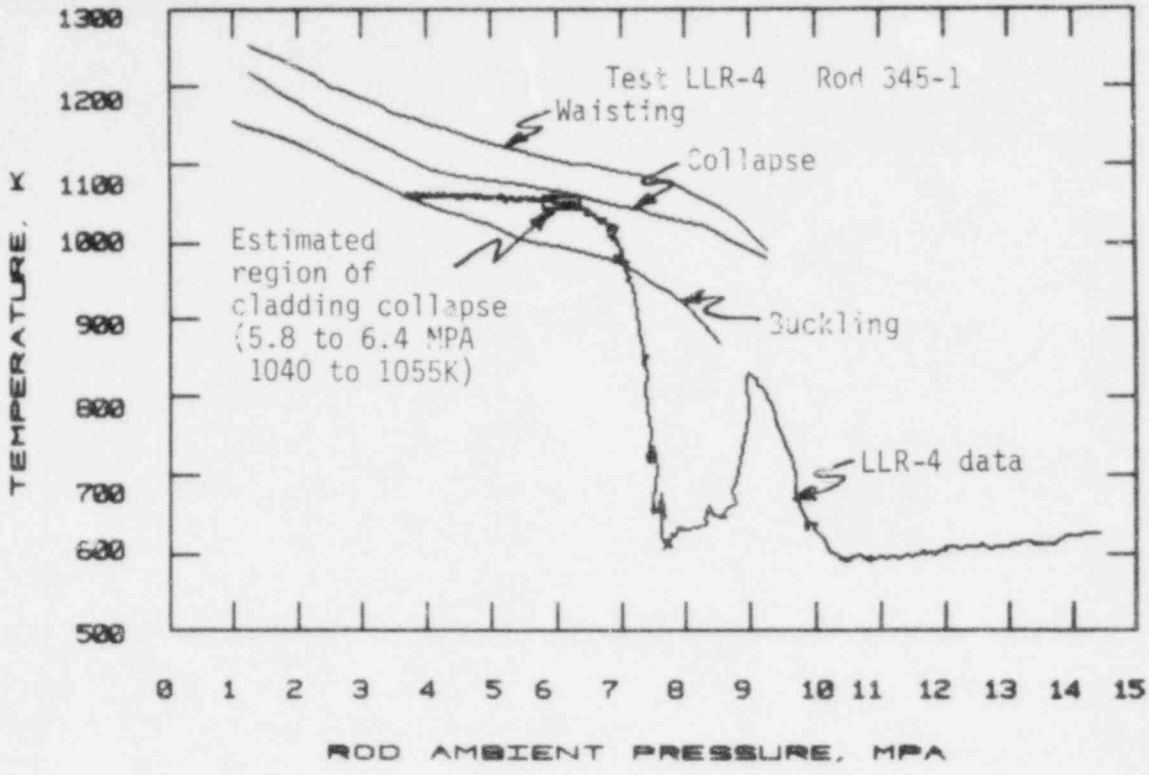


Figure 18 A comparison of measured cladding temperature and external pressure with cladding deformation data. The region indicated defines the temperature and pressure that probably resulted in collapse. Rod 345-1, test LLR-4.

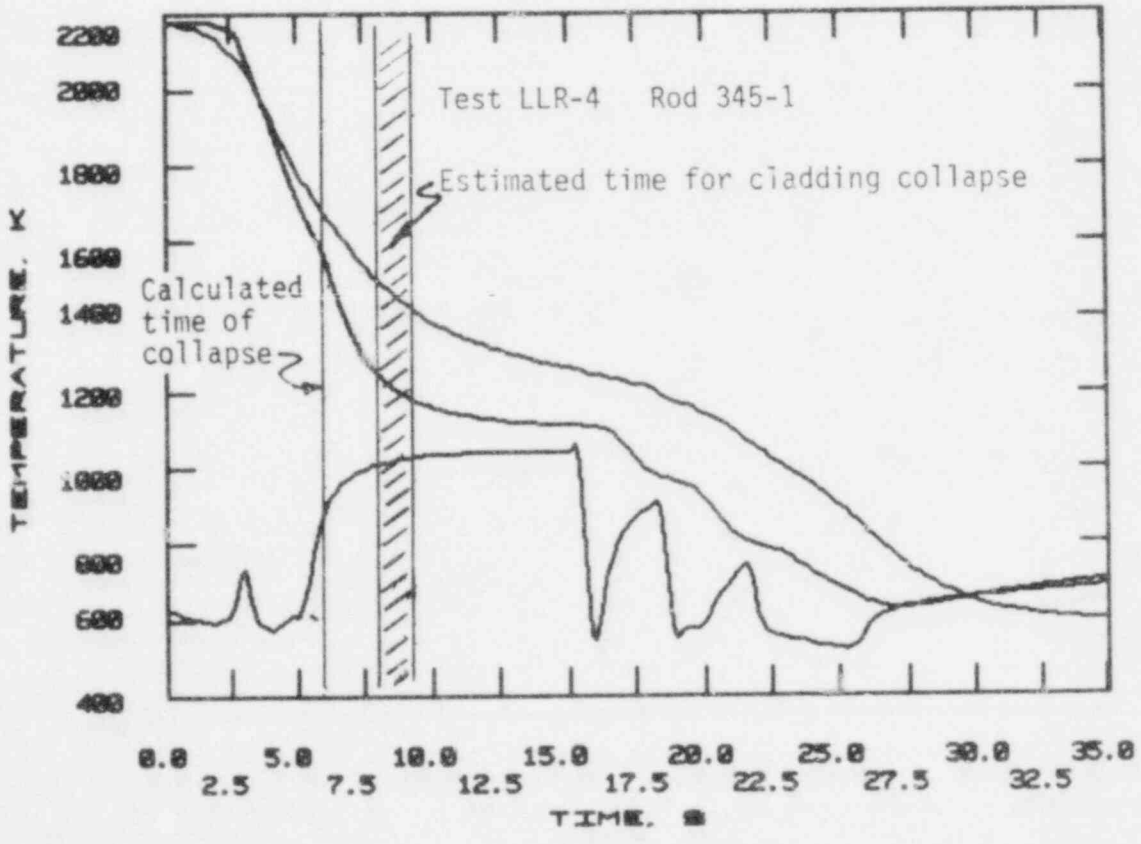


Figure 19 Calculated and measured data for fuel rod 345-1, test LLR-4; indicating the time FRAP-T5 calculated collapse and an estimated time of actual collapse.

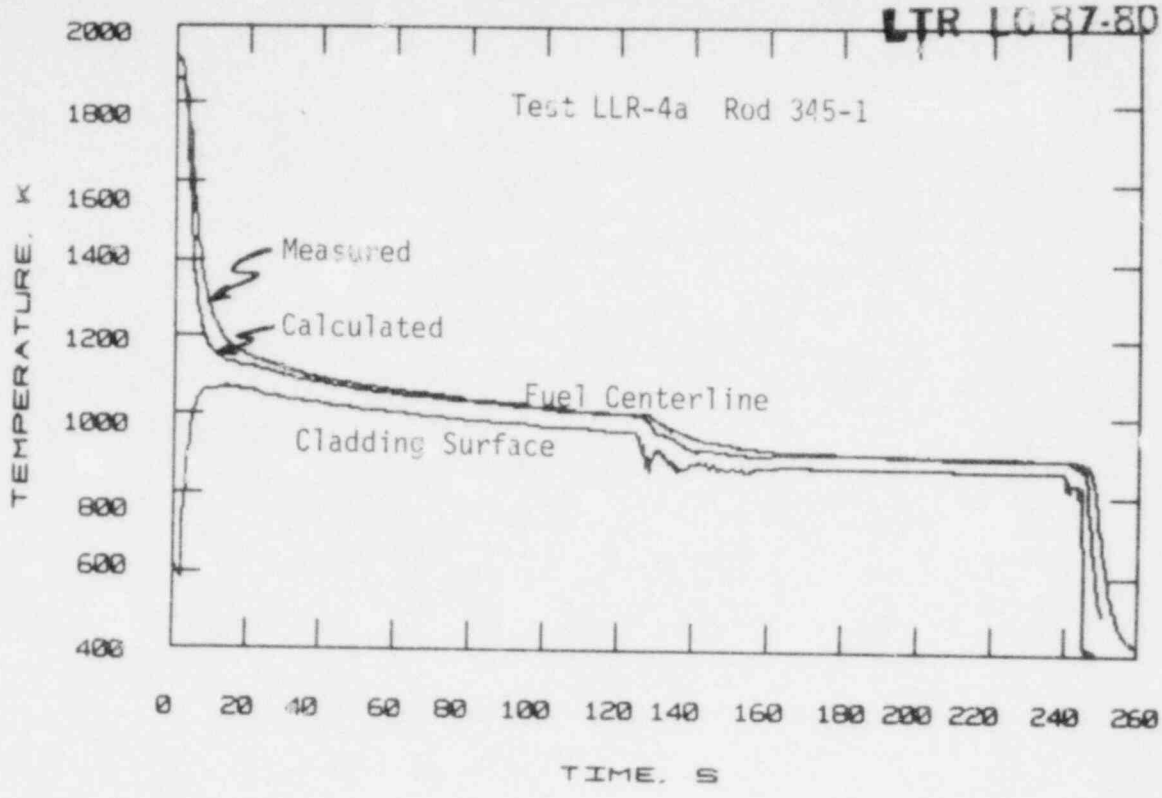


Figure 20 Calculated and measured centerline temperature with an overlay of the measured cladding surface temperature. Fuel rod 345-1, test LLR-4a.

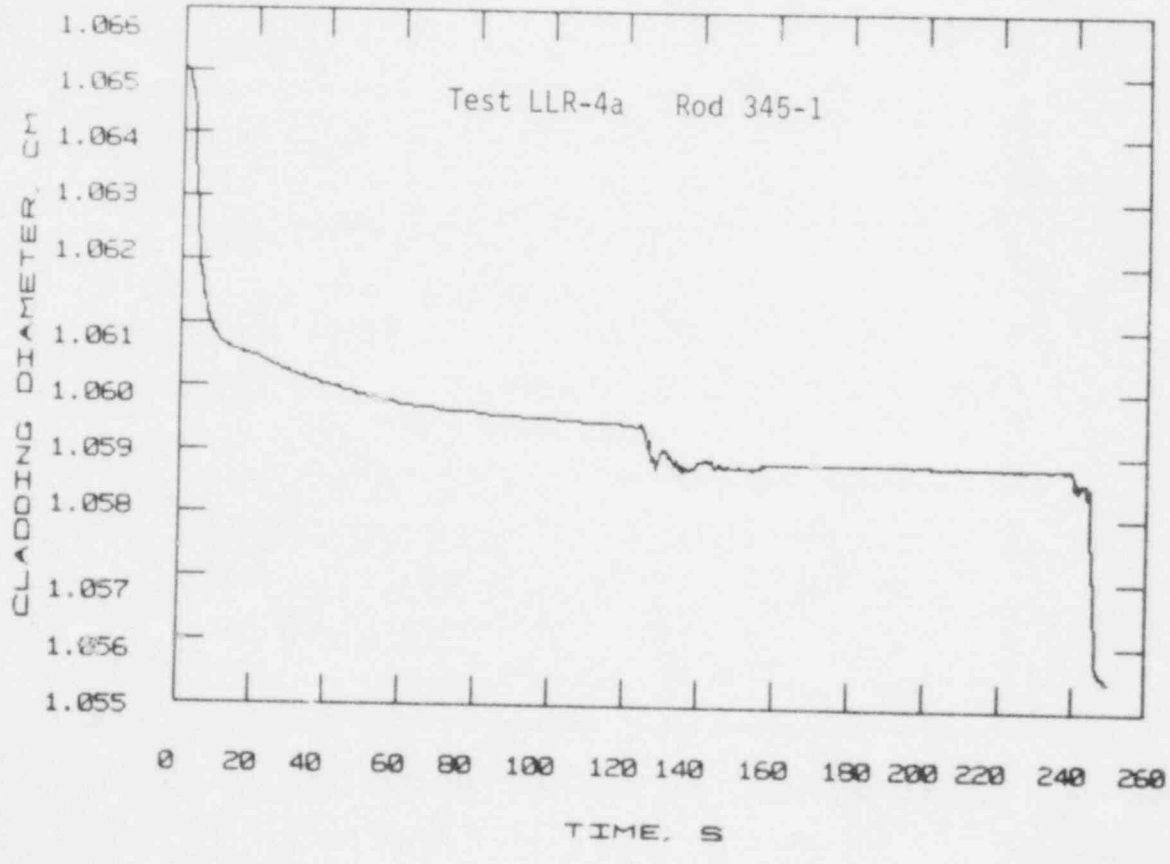


Figure 21 Calculated cladding OD corresponding to the data in Figure 20.

included for comparison. During the steady-state operation prior to blowdown, the measured centerline temperature was approximately 1920 K compared to a calculated value of 1865 K. Reactor scram for this test was delayed 2.8 seconds after initiating blowdown. The centerline temperature response for rod 345-1 to the LLR-4a transient was typical of the responses observed in the previous tests, i.e., the temperature remains essentially constant for the first two seconds as the power level and surface heat transfer remain close to the preblowdown values. After CHF and film boiling occurs, and after the power level has dropped, the centerline temperature decreases rapidly as the fuel enthalpy is redistributed within the fuel rod. At approximately 15 s, the redistribution is nearly complete and the decline in the centerline temperature slows to a rate indicative of continued film boiling and radiation heat transfer.

The FRAP-T5 calculation for test LLR-4a, rod 345-1 was initialized from the end-of-test conditions calculated for the previous LLR-4 test, which included collapsed cladding. The calculated centerline temperature response is included in Figure 20. The initial steady-state temperature was calculated to be 1865 K; 55 K lower than the measured value. The temperature without collapsed cladding was calculated to be approximately 2120 K (Refer to Figure 6) which is a good indication the cladding had collapsed during the LLR-4 test. The initial cladding OD for this case was about 0.09 mm less than the diameter for a nominal BOL fuel rod. The difference in cladding diameters can be seen by comparing the data in Figure 13 with that in Figure 21. Figure 21 shows the cladding response calculated for the LLR-4a test. At the time blowdown is initiated, the pellet and cladding are in hard contact and the interfacial pressure is calculated to be 51.6 MPa. The pressure drops very rapidly to approximately 4.3 MPa at four seconds as the cladding responds to the increase in temperature and reduction in coolant pressure. Between 4 and 18 s the pellet-to-cladding interfacial pressure remains essentially constant (4 to 7 MPa) and at 18 s begins a slow decline, reaching zero at 46 s. At the time of blowdown, the gap conductance is calculated to be 61.4 $kW/m^2$-K and remains essentially at this value to 37 s where it descends to 33.4 $kW/m^2$-K at 46 s.

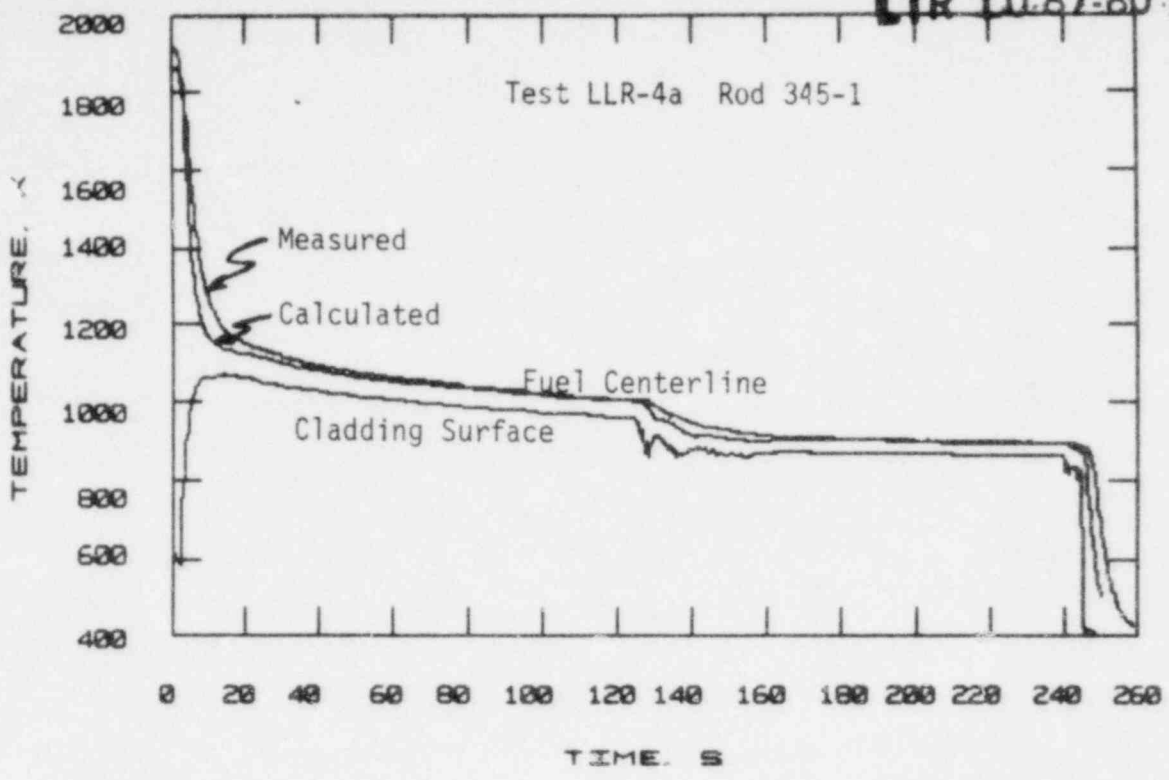


Figure 20 Calculated and measured centerline temperature with an overlay of the measured cladding surface temperature. Fuel rod 345-1, test LLR-4a.

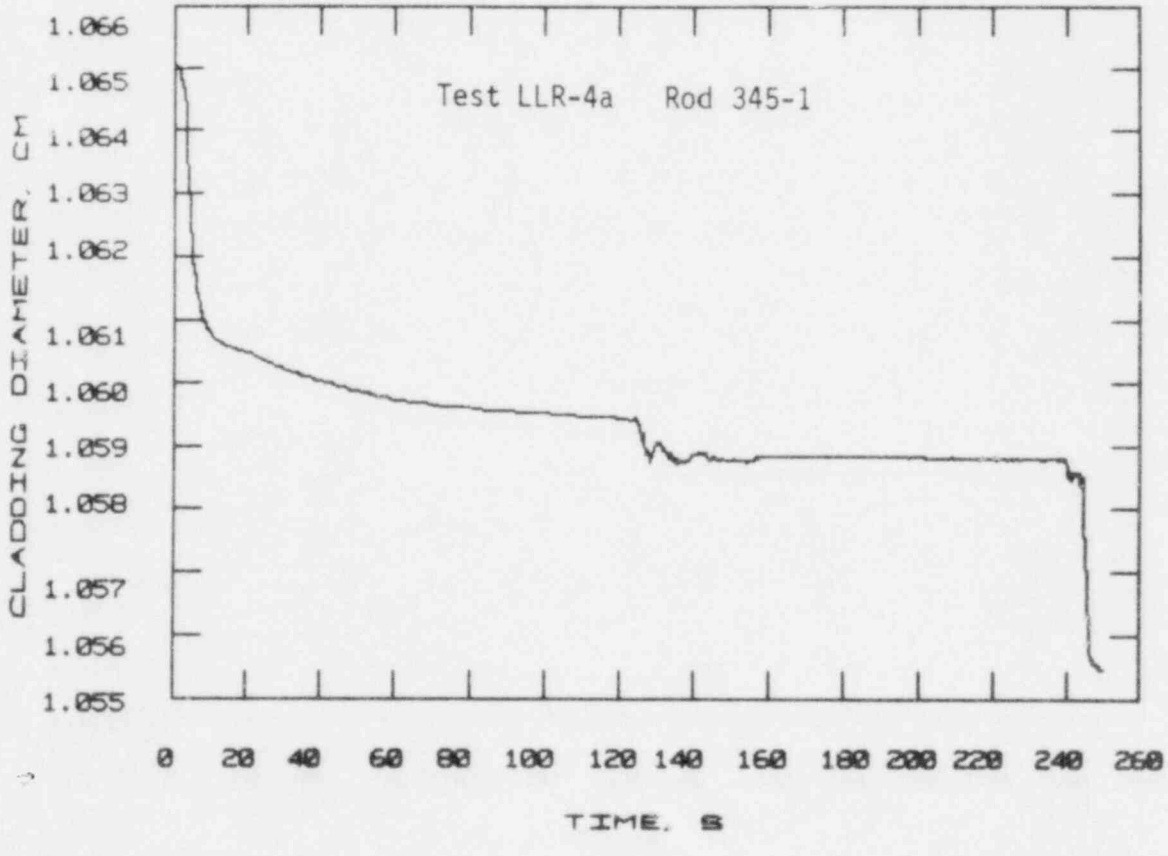


Figure 21 Calculated cladding OD corresponding to the data in Figure 20.

Referring to Figure 20, it is noted that the difference in the initial (steady-state) measured and calculated centerline temperature is approximately 55 K. At three seconds, the calculated data begin to diverge and become less than the measured data. At five seconds, the difference has increased to about 190 K and then begin to converge, attaining the initial difference of 55 K at 15 s. The relative calculated-to-measured response observed here indicates that the calculated fuel rod thermal resistance is too small between the 3 to 5 s interval. Figure 21a shows the same calculated cladding diameter as Figure 21 but with an expanded time scale to show more detail. From this figure, the calculated cladding diameter is seen to begin a rapid decrease at approximately three seconds. Apparently the calculated cladding temperature has attained the threshold for plastic deformation and for the next few seconds, the cladding follows the diameter of the pellet that has started to cool. It was concluded previously (Section 5.1.4) that FRAP-T5 probably predicts cladding collapse or plastic deformation before it actually occurred. Again, the results of the LLR-4a calculation supports this conclusion, i.e., if the onset of cladding deformation calculated by FRAP-T5 was delayed 1 to 2 s, the calculated thermal resistance would have been larger and consequently the centerline temperature in the 3 to 5 s interval would have been in better agreement with the data.

Another possible explanation for the difference in the measured and calculated centerline temperature responses is that FRAP-T5 could be calculating a fuel rod thermal resistance that is too small for a collapsed cladding situation. Since the LLR-4a test was initiated with collapsed cladding, this would account for the initial or preblowdown difference. In addition, there were indications the code was overestimating thermal resistance for the collapsed cladding situation during the coolant transients in LLR-4 test (Refer to Section 5.1.3).

Based on the comparisons of centerline temperature response calculated by FRAP-T5 and the measured data, the following conclusions are made

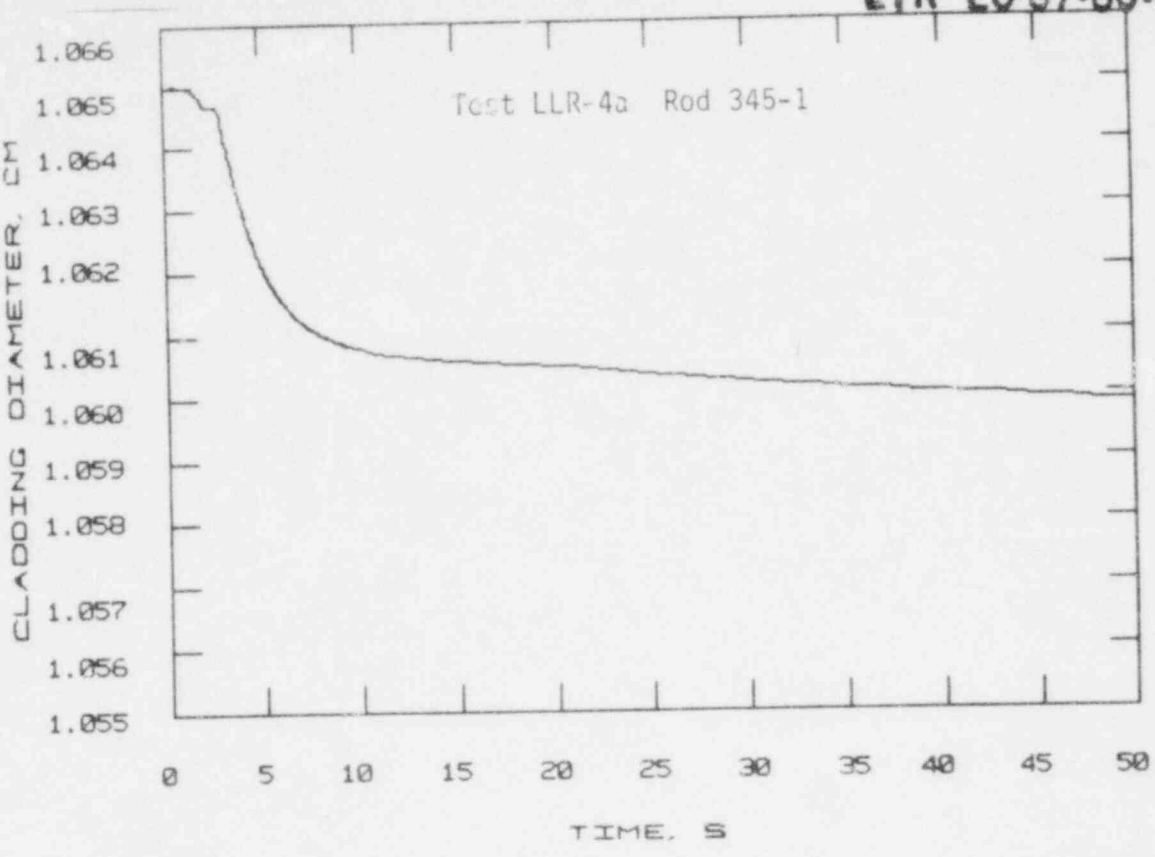


Figure 21a Same data as Figure 21 with an expanded time scale, 0 to 50 s time interval.

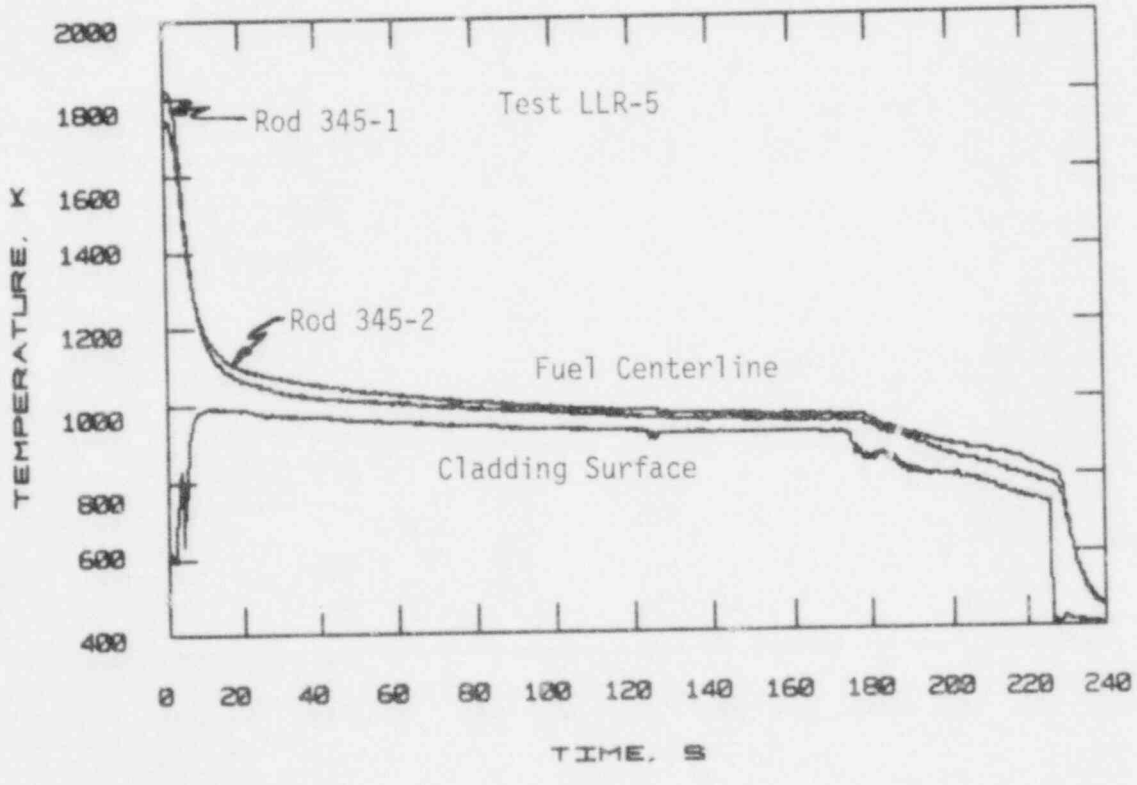


Figure 22 An overlay of the measured centerline temperature from fuel rod 345-2 and the measured centerline and cladding surface temperatures from fuel rod 345-1. Test LLR-5.

regarding the capability of the code to predict cladding collapse and calculate transient centerline temperatures.

(1) FRAP-T5 predicted cladding collapse before it occurred in the LLR tests. The threshold for cladding deformation defined in the code appears to be at less severe conditions than required for collapse.

(2) The calculated centerline temperature for a collapsed cladding situation does not agree with the data as well as the calculation for noncollapsed cladding. The reason may be that FRAP-T5 calculates cladding deformation at less severe conditions than necessary and/or the code calculates thermal resistances that are too small for a collapsed cladding situation.

It is concluded, therefore, that FRAP-T5 will provide a conservative estimate of the LOFT cladding deformation and could be useful in requalification of the LOFT core for additional tests.

## 5.2 Surface Thermocouple Effects Based on Centerline Temperature Analysis

The thermocouples (TC) on the cladding surface are suspected of producing a fin effect and thereby increasing the cooling of the fuel rod. During the blowdown phases of a LOCE, it is postulated that this TC effect could delay CHF, which would reduce the magnitude of the subsequent cladding temperature transient. Also, during the reflood or cooling phase of the LOCE, the surface thermocouples could cause fuel rods to cool faster and possibly quench at an earlier time than fuel rods without thermocouples. It is possible that both the delayed CHF and the faster cooldown and quench during reflood would be reflected in the centerline temperature response. The centerline temperature data obtained during the LLR tests were, therefore, reviewed for evidence of increased cooling of the fuel rod as a result of the surface thermocouples. The results of that review are presented here.

As indicated previously, test fuel rod 345-1 had surface thermocouples whereas rod 345-2 did not. Both rods had centerline thermocouples and both rods were placed in the test series at the same time. The location of the centerline TCs were slightly different; 0.533 and 0.457 m above the bottom of the active fuel for rods 345-1 and 345-2 respectively. Both elevations are near the axial power peak and the maximum difference observed from flux wires irradiated during the LLR test was approximately four percent. Regardless of this, the centerline temperature measured prior to initiating blowdown was consistently higher (59 to 235 K) for rod 345-1. Since the postulated surface TC enhanced cooling effect would be small or nonexistant at normal steady-state operation, these differences in steady-state temperatures are probably the result of effects other than surface thermocouple installation. For example, the rod average power may have been larger, or there may be a TC accuracy contribution and possibly the thermal resistance across one fuel rod differs from that of the other. For this transient analysis, however, only relative changes in the centerline temperature and the time these changes occur will be considered.

Fuel rods 345-1 and 345-2 were installed for the LLR-5 test and were included in the remainder of the test series. Consequently the data analysis presented here includes tests LLR-5, LLR-4 and LLR-4a.

5.2.1 Test LLR-5. The centerline temperature response obtained from rods 345-1 and 345-2 and the cladding surface temperature obtained from rod 345-1 are shown in Figure 22 for the LLR-5 blowdown and reflood. The time scale was expanded in Figures 22a and 22b to show greater detail of the respective blowdown and reflood phases of the test. Referring to Figure 22a, the centerline temperature for rod 345-2 is observed to increase slightly in the zero to one second interval indicating that CHF and film boiling may have occurred prior to reactor scram (the reactor was scrammed at approximately two seconds), whereas the centerline temperature for Rod 345-1 is essentially constant for the same time interval. CHF at the location of the surface TC on rod 345-1 did not occur until approximately two seconds; thus indicating a possible delayed CHF due to the surface thermocouples.

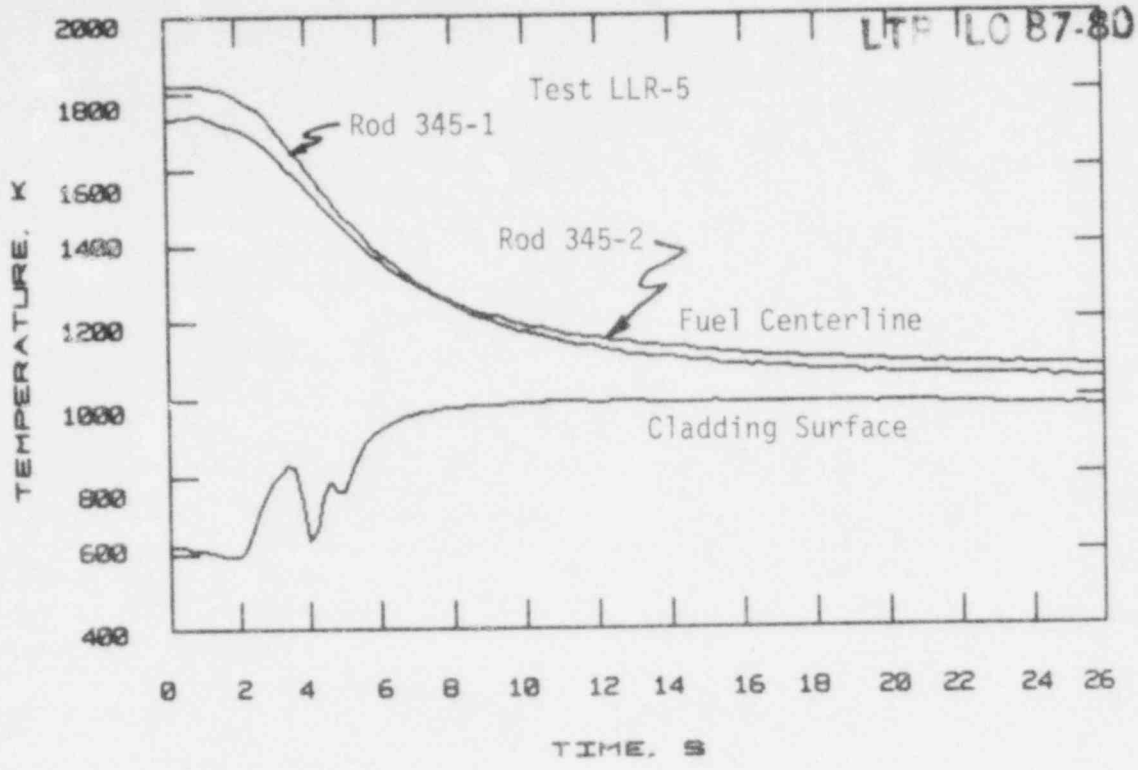


Figure 22a Same data as Figure 22 with an expanded time scale, 0 to 26 s time interval.

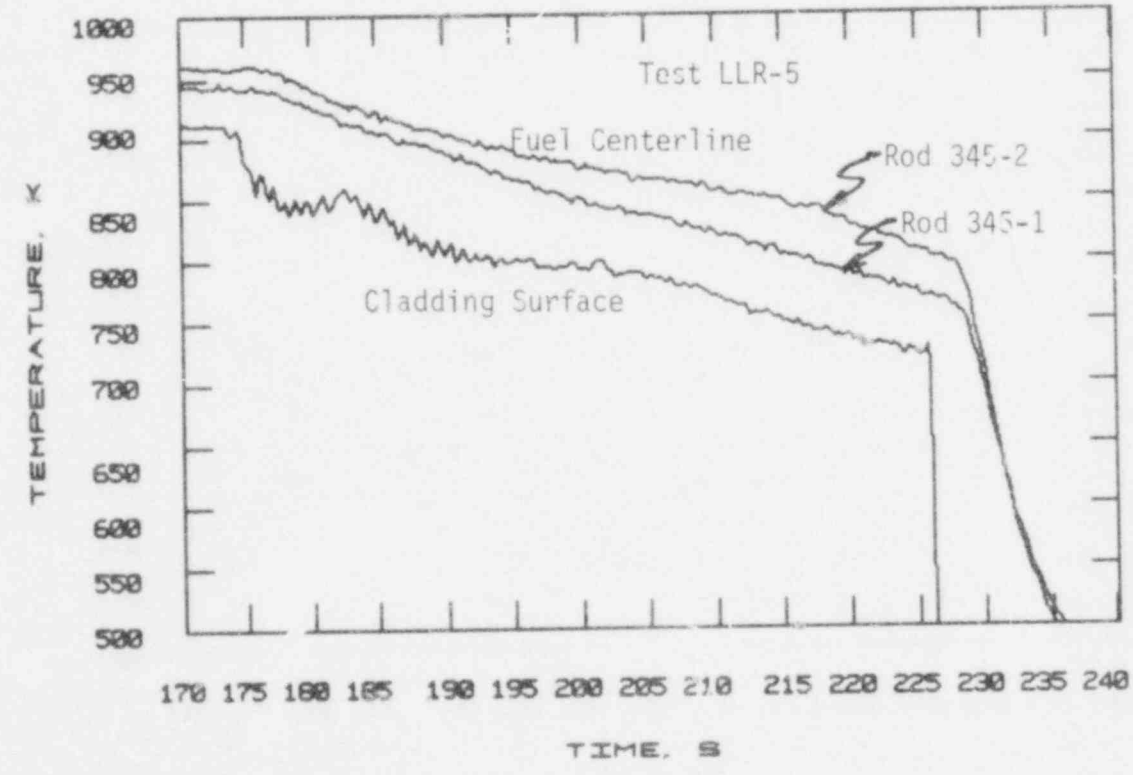


Figure 22b Same data as Figure 22 with an expanded time scale, 170 to 240 s time interval.

In the 2 to 26 s time interval, the centerline temperature data in Figure 22a show the temperature for rod 345-1 decreasing at a faster rate than the data for rod 345-2. Although this is indicative of greater cooling and a possible TC effect, there is evidence that the coolant thermal-hydraulics in the channel for rod 345-1 were different and provided more cooling. The cladding surface temperature data for rod 345-1, provided in Figure 22a, clearly shows a cooling transient occurred between three and four seconds. The other TC on rod 345-1 (0.533 m elevation, 180° azimuthal) also shows the same phenomenon. Of the four other surface thermocouples involved in this test (2 each on rods 312-1 and 312-2), only one (rod 312-2, 0° azimuthal) showed signs of a cooling transient and to a much lesser degree than the data from rod 345-1. Thus, the more rapid decline in the centerline temperature for rod 345-1 may, at least in part, be a result of differing thermal-hydraulic conditions in the flow shroud. The lower turbine in coolant channel for rod 345-2 had failed during this test and consequently different thermal-hydraulics could not confirmed.

After the initiation of reflood (approximately 175 s), the centerline temperature for rod 345-1 again decreases at a faster rate than the corresponding data for rod 345-2 as shown by the data in Figure 22b. The centerline temperature data in Figure 22b also indicate that the fuel rods quenched at essentially the same time. Since reflood is from the bottom and the centerline TC in rod 345-1 is 7.6 cm further up the channel, rod 345-2 would be expected to quench first; everything being equal. The faster decline in the centerline temperature for rod 345-1 after initiation of reflood and the same quench times suggests a possible surface TC effect.

Although the relative centerline temperature response from the LLR-5 test is indicative of a possible TC effect, the observed response may also be the result of differences in the coolant thermal-hydraulics. Also any errors associated with TC calibration may have contributed. At any rate, the general response of the two rods is very similar, and the data suggests that if TC effects are present, they change the general response of the rod.

5.2.2 Test LLR-4. The measured centerline temperature data for rods 345-1 and 345-2 and the cladding surface temperature for rod 345-1 (0° azimuthal) are shown in Figure 23 for the LLR-4 test. At approximately 30 s, the fuel centerline temperature for rod 345-1 drops below the cladding surface temperature and for the next 40 s oscillates about the cladding temperature. At about 7 s, the centerline temperature again drops below the cladding temperature and begins a rapid descent; declining to approximately 150 K (-123C) at 100 s. In an effort to explain this anomaly, the source of the data and the calibration factor applied were checked. The records show that the questionable data were from the centerline TC for rod 345-1 and that the calibration factor was the same used for both the preceding and succeeding tests where the data appear to be correct. The data from this instrument prior to nuclear operation, but with the coolant at operating conditions (~600 K), was indicating a temperature of approximately 600 K. Similarly, the corresponding data from this instrument for the following test, LLR-4a, is again indicating a temperature of approximately 600 K. In addition the posttest calibration of the data acquisition electromics showed no abnormality. At the time of this writing, no information has been found to adequately explain this anomly in the data.

During a loss-of-coolant experiment in PBF, conditions would not exist where the fuel centerline temperature would become less than the temperature at the cladding surface. Therefore, the centerline temperature response for rod 345-1 shown in Figure 23 is known to be in error after 30 s and only the first 25 s of data will be used in the analysis presented here.

To provide more detail during the blowdown phase, the data in Figure 23 is shown in Figure 23a with an expanded time scale. From these data, the centerline temperature for rod 345-2 is observed to increase slightly for the first half second whereas the corresponding data for rod 345-1 starts an immediate decline. Since rod 345-1 had the surface thermocouples, this relative response could be caused by increased cooling occuring at the location of the surface TC, and a delayed CHF.

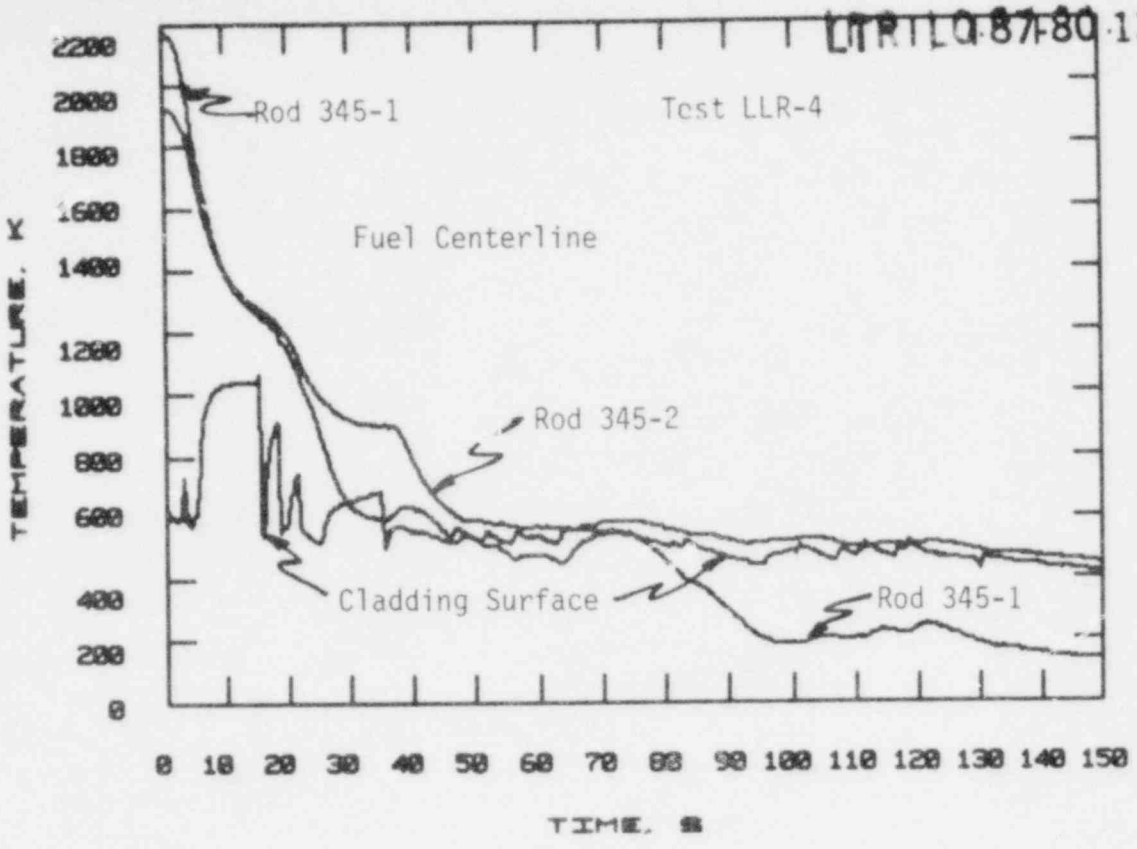


Figure 23 An overlay of the measured centerline temperature from fuel rod 345-2 and the measured centerline and cladding surface temperature from rod 345-1, test LLR-4.

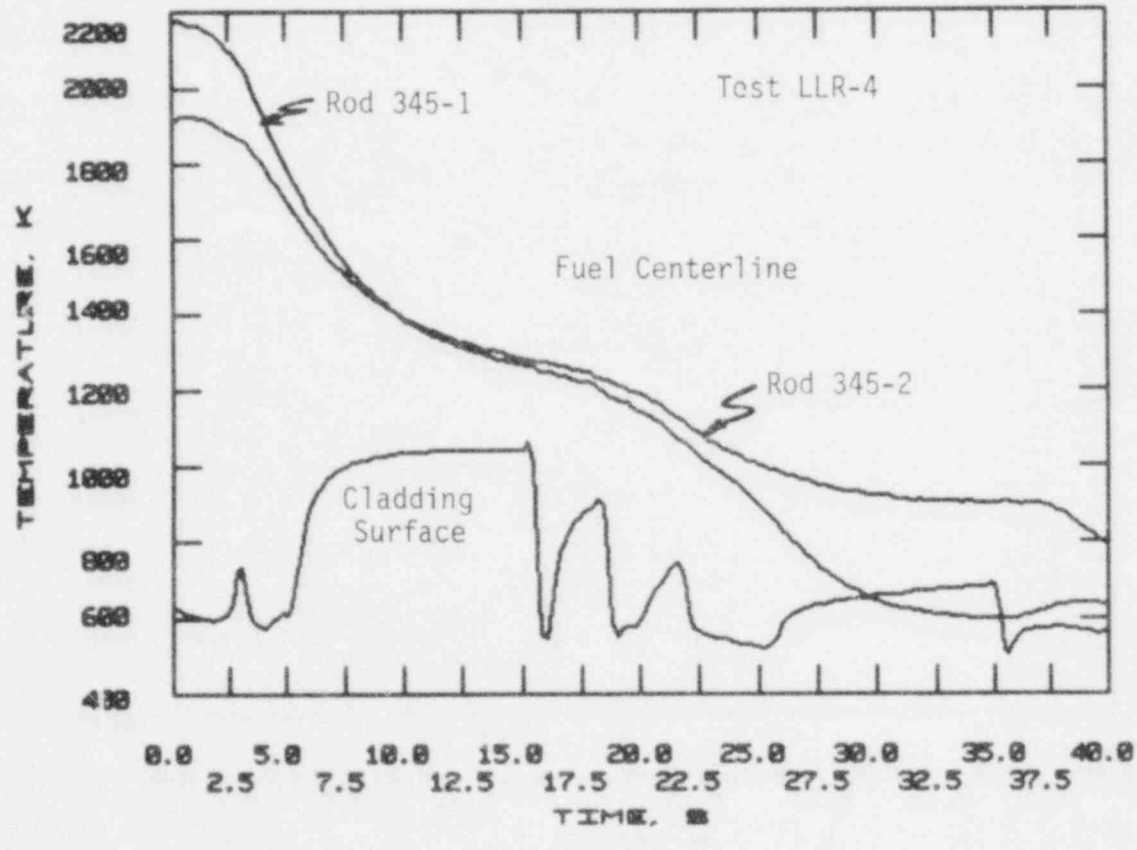


Figure 23a Same data as in Figure 23 with an expanded time scale, 0 to 40 s time interval.

Differences in the coolant thermal-hydraulics appear to have occurred a short time later in the blowdown. At about 2 to 2.5 s, the cladding temperature data in Figure 23a indicate rod 345-1 experienced CHF, started into film boiling and was suddenly cooled before stable film boiling was achieved. The other TC on this rod also shows the same response. The surface TCs on rods 312-1 and 312-2, however, do not indicate that this cooling transient occurred. It is possible therefore, that the coolant transient did not occur for rod 345-2 and was unique to rod 345-1. The coolant transient is believed to have been caused by the malfunction of the check valve located on the upper end of the coolant shroud for rod 345-1. The lower turbine flowmeter for rod 345-2 remained out of commission for this test and consequently conformation that the coolant-transient was unique to rod 345-1 cannot be made.

The centerline temperature for rod 345-1 continues the faster decline for approximately 7.5 s, as shown by Figure 22a. Although this may result from enhanced cooling by the surface TCs, it also may result from the different coolant thermal-hydraulics discussed above.

Between 7.5 and 16.0 s, the centerline temperatures in Figure 23a appear to be decreasing at about the same rate. At 16 s, however, the data begin to diverge, with the temperature from rod 345-1 again decreasing at a faster rate. The diverging temperatures coincides with a series of cooling transients, which are reflected in the cladding surface temperature data in Figure 23a, and are caused by a series of inadvertent opening and closing of a system isolation valve that allowed coolant to enter the test space. These cooling transients occurred for all four fuel rods and it is not possible to determine that fuel rod 345-1 received more coolant than rod 345-2. Although the faster declined observed in the centerline temperature from rod 345-1 is indicative of a surface TC effect, it may also have been the result of different thermal-hydraulics. Also, the response of the centerline TC for rod 345-1 is questionable because of the abnormal data recorded after 75 s. Consequently, the relative response observed may be the result of thermocouple error.

5.2.3 Test LLR-4a. The fuel centerline temperature data for rods 345-1 and 345-2 and the cladding surface temperature data for rod 345-1 are illustrated in Figure 24 for the LLR-4a test. Again, the time scale has been expanded in Figures 24a and 24b to show more detail during the respective early blowdown and reflood phases.

Referring to Figure 24a, the centerline temperature response for rod 345-2 does not show the initial (0 to 1 s) increase that was observed for the two previous tests. In addition, the early cooling transient occurring for rod 345-1 during the 2.5 to 4.0 s interval of tests LLR-5 and LLR-4 was not observed in the cladding TC data for this test. Also, the flow data from the inlet flow turbine for rods 345-1 and 345-2, shown in Figure 25, do not show a significant difference in the coolant supplied to these two rods. The early rewet coolant transient[a] observed in tests LLR-5 and LLR-4, in conjunction with the initial increase in the centerline temperature for rod 345-2 which are missing in this test (LLR-4a), implies that the delayed CHF postulated for rod 345-1 during the LLR-5 and LLR-4 tests may have been caused by the cooling transient and not a TC effect. On the other hand, the relative temperature response between 2 to 20 s, which is similar for all three tests and which was postulated to have been caused by the cooling transient in tests LLR-5 and LLR-4, would now be considered a TC effect. (The relative response in the 2 to 20 s time interval indicated the centerline temperature for rod 345-1 to be decreasing faster than the corresponding temperature for rod 345-2. Refer to Figures 22a, 23a and 24a.)

Although the inlet turbine data in Figure 25 indicates the coolant flow is essentially the same for both fuel rods, more effective cooling may occur at the location of the centerline TC for rod 345-1 than at the location of the TC for rod 345-2. The direction of the coolant flow during

---

a. The early cooling transient occurring during tests LLR-5 and LLR-4a was caused by a leaking check valve on the flow shroud for rod 345-1. The value was repaired prior to the LLR-4a test.

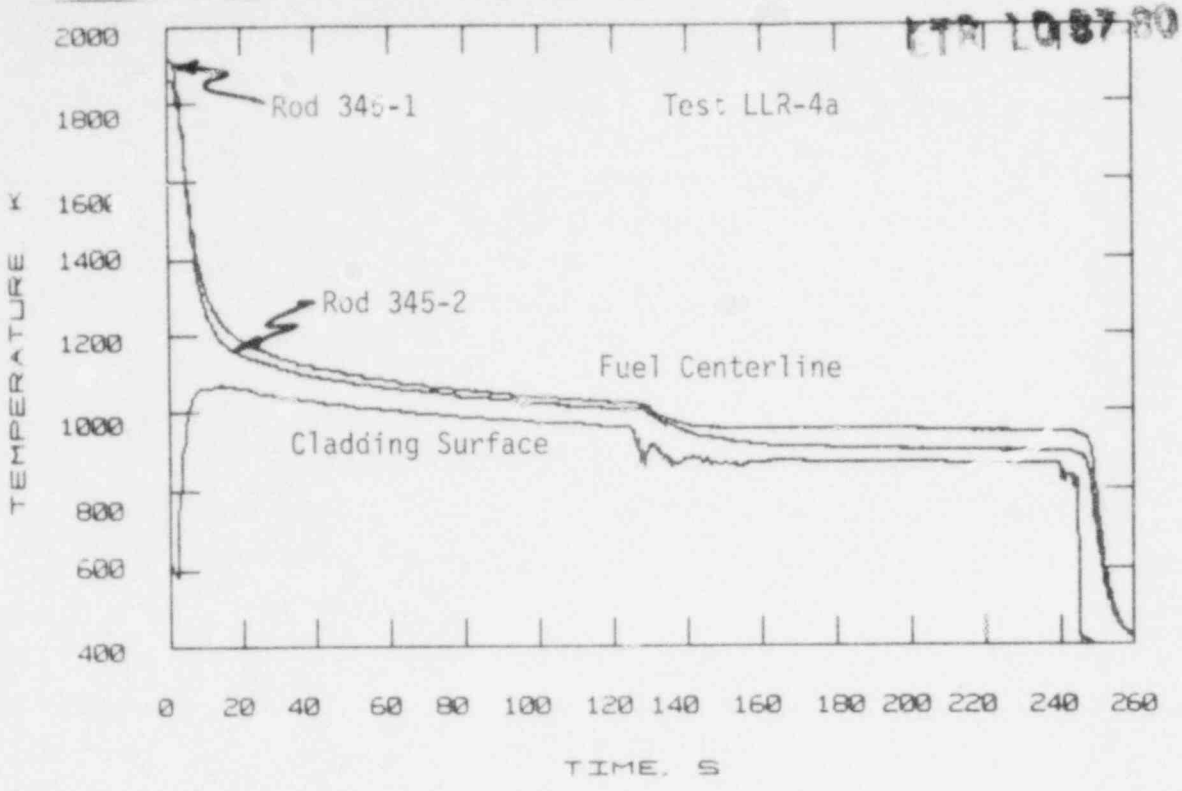


Figure 24 An overlay of the measured centerline temperature from fuel rod 345-2 and the measured centerline and cladding surface temperature from rod 345-1, test LLR-4a.

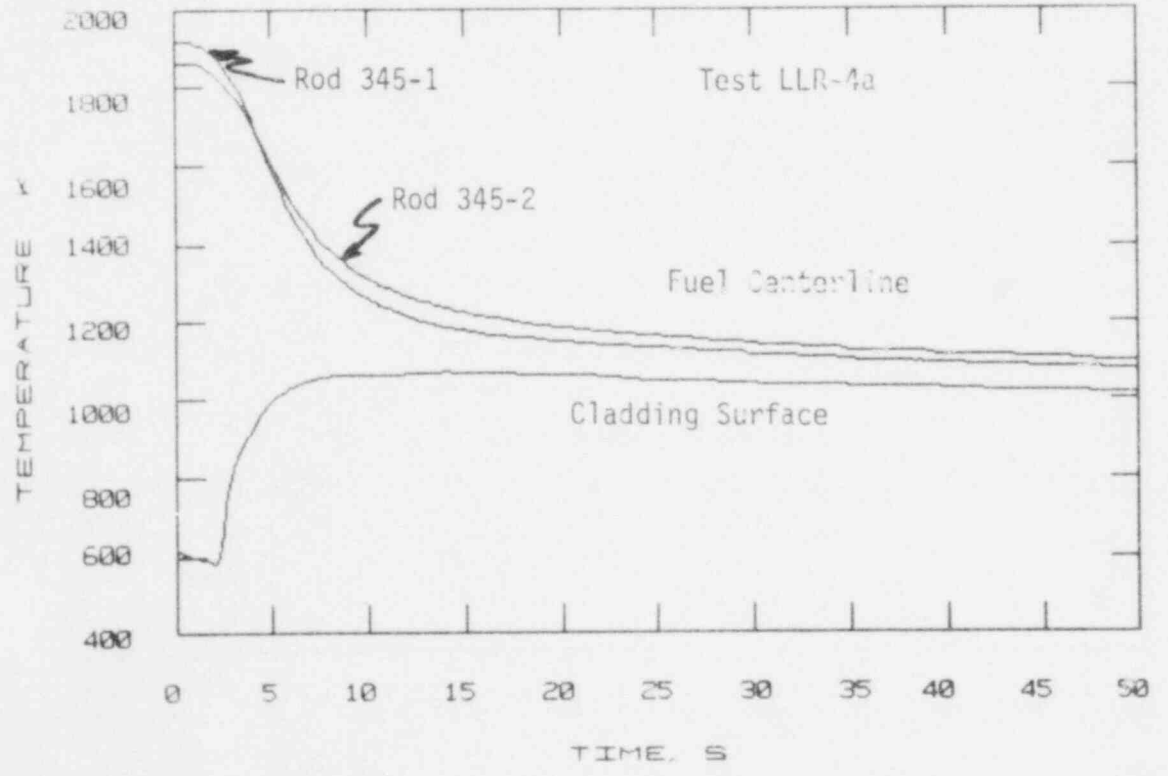


Figure 24a Same data as in Figure 24 with an expanded time scale, 0 to 50 s time interval.

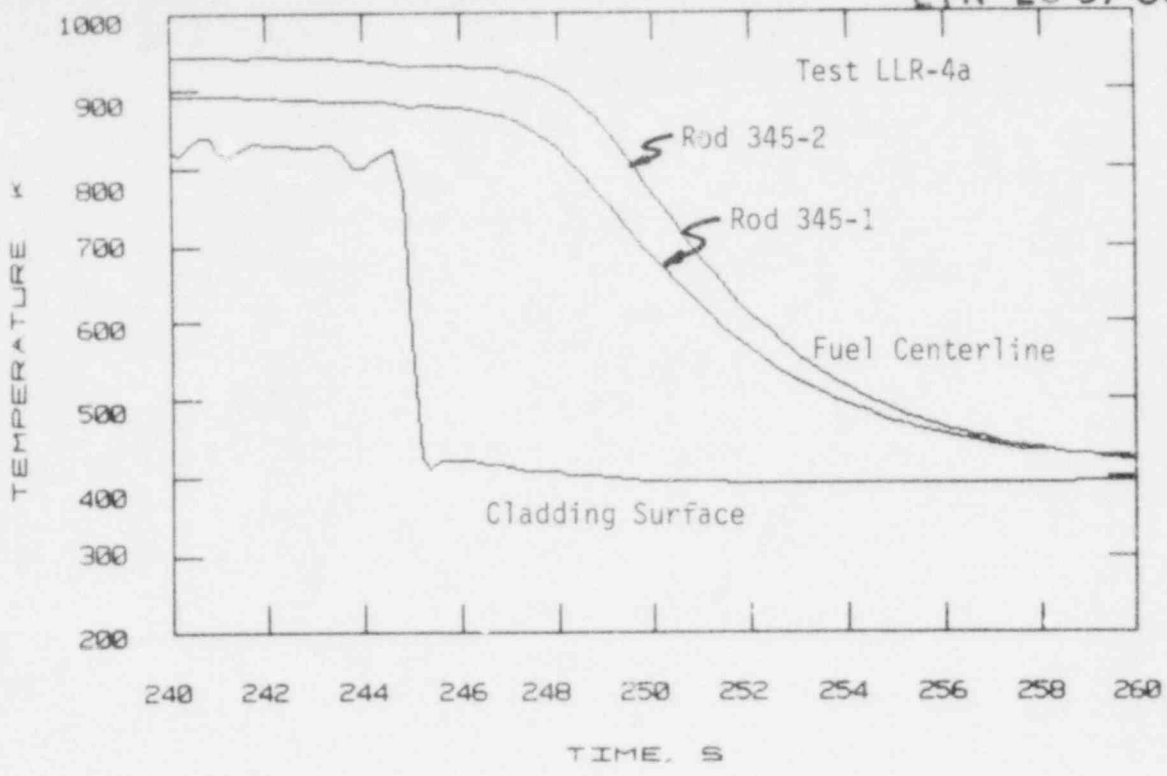


Figure 24b Same data as in Figure 24 with an expanded time scale, 240 to 260 s time interval.

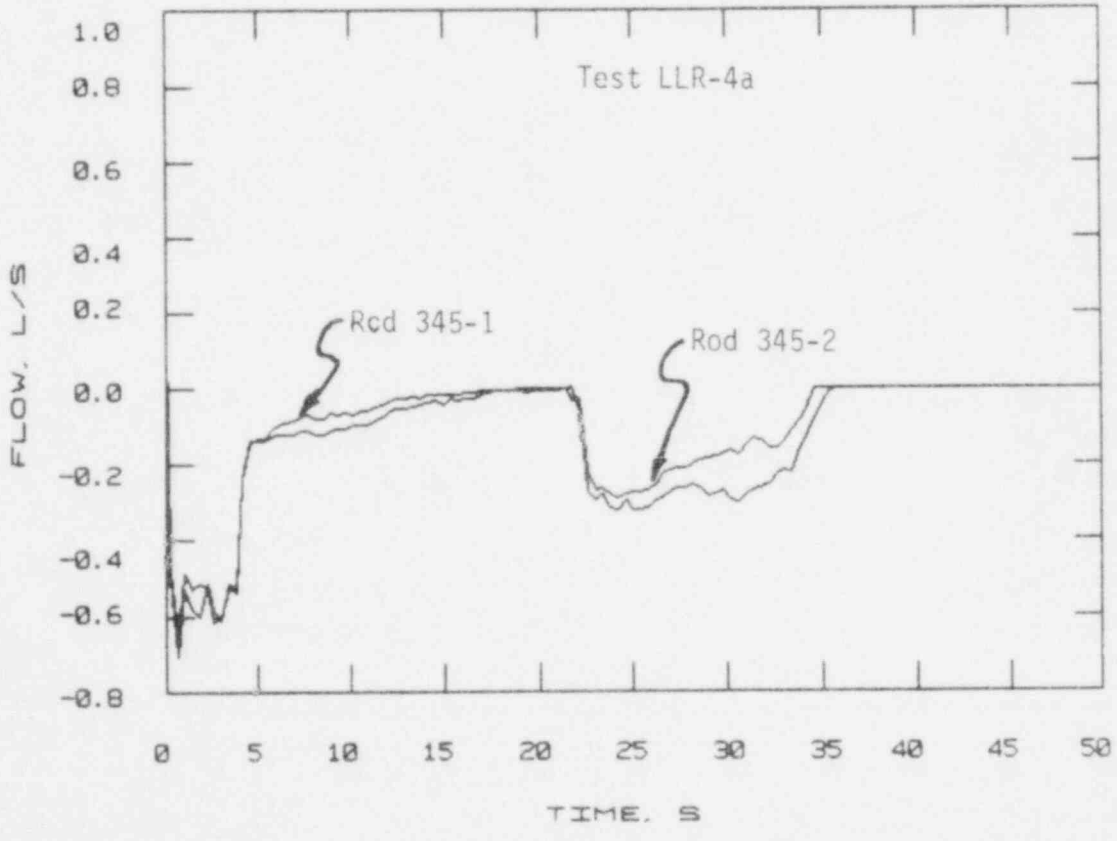


Figure 25 Measured volumetric coolant flow at the lower shroud elevation for fuel rod 345-1 and 345-2, test LLR-4a, 0 to 50 s time interval.

the early stages of blowdown is downward or reversed as shown by Figure 25. Since the TC for rod 345-2 is approximately 7.6 cm below the TC for rod 345-1, the coolant quality would be slightly greater and consequently provide less effective cooling. Thus, the difference in the centerline temperature response in the 2 to 20 s interval may still be the result of different cooling conditions and not a TC effect.

Reflood for the LLR-4a test was initiated at approximately 120 s and is reflected in the cladding surface temperature shown in Figure 24. A few seconds after reflood, the centerline temperature for rod 345-1 is again observed to decline at a faster rate. Since reflood coolant is from the bottom, i.e., upward flow, an indication of the relative flow between channels can be obtained from the inlet and outlet turbins. These flow data are provided in Figures 26 and 27, respectively on a 100 to 260 s time scale. Although the inlet turbines indicate the inlet flow for both rods were essentially the same, the outlet turbines indicate that the flow for rod 345-2 may have been slightly greater. Thus, rod 345-2 may have received more coolant, yet rod 345-1 is being cooled faster. In addition, the centerline temperature response in Figure 24a shows that rod 345-1 was quenched sooner although the centerline TC was approximately 7.6 cm further up the channel. Therefore, the relative centerline temperature response for rods 345-1 and 345-2 observed during the reflood and quench phase of test LLR-4a are indicative of the response expected if a TC effect was present.

The following observations are summarized from this analysis of the centerline temperature response obtained from rods with and without surface thermocouples:

(1) The relative centerline temperature response from fuel rods with and without surface thermocouples is similar for all three tests and this relative response could be considered to be caused by the surface thermocouples.

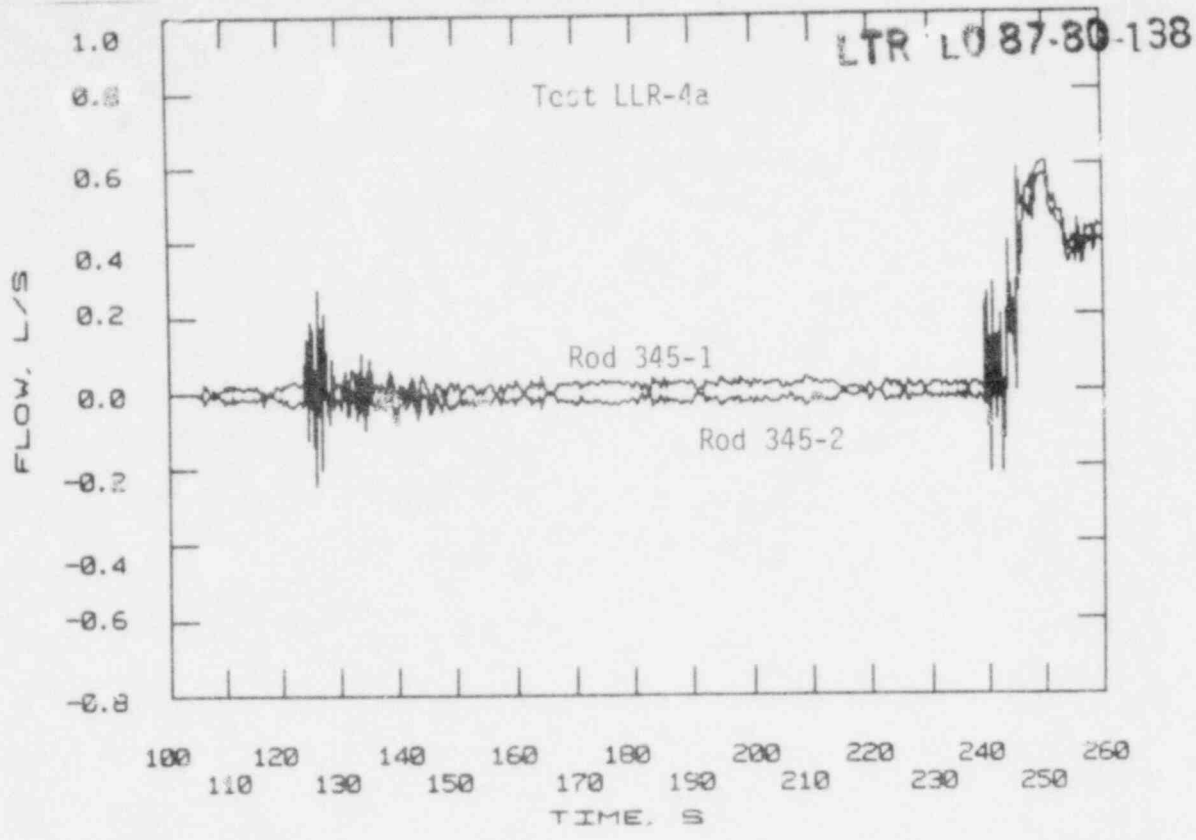


Figure 26 Measured volumetric coolant flow at the lower shroud elevation for fuel rod 345-1 and 345-2, test LLR-4a, 0 to 50 s time interval.

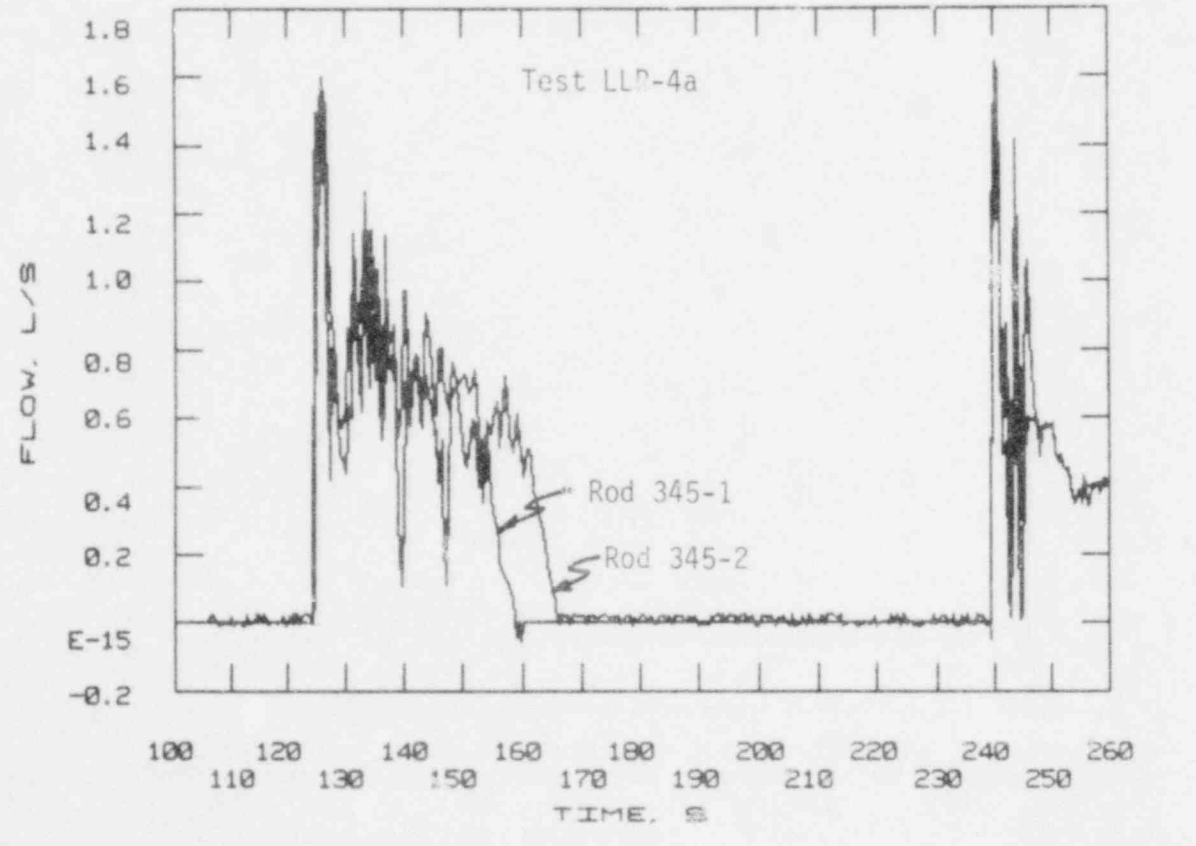


Figure 27 Measured volumetric coolant flow at the upper shroud elevation for fuel rod 345-1 and 345-2, test LLR-4a, 100 to 260 s time interval.

(2) The relative response obtained from two tests, LLR-5 and LLR-4, are suspected of being complicated by differences in the coolant thermal-hydraulics.

(3) The centerline temperature for rod 345-1, test LLR-4, drops below the measured cladding temperature, which is not in accordance with any conceivable behavior, and since the information explaining this anomaly is not available, all data from this TC must be questioned.

(4) The relative temperature response observed during the LLR-4a test is not complicated by other, easily identifiable effects and, therefore, could be considered as a possible TC effect.

(5) The data considered in this analysis were the relative centerline temperature response between the same two fuel rods. Differences observed in the centerline temperature may, therefore, be the result of inherent characteristics of the fuel rods.

Although the relative centerline temperature responses are indicative of the response expected for TC effects, it is not possible to establish a definite TC effect from these data. The inability to determine the exact cause for the abnormal data obtained from the centerline TC for rod 345-1 during the LLR-4 test requires that all data from this instrument be suspected of error. In addition, the small quantity of data reviewed consisted of the relative centerline temperature response between two fuel rods. Thus, the possible surface TC effect observed may actually be the result of characteristics inherent to the fuel rods; e.g., TC calibration and differences in the thermal resistance between the two fuel rods. Futhermore, differences in the thermal-hydraulic conditions are known to have existed for two tests, LLR-5 and LLR-4.

# 6. CONCLUSIONS

Based on the analysis of the steady-state data from the LLR tests, it is concluded there is evidence to support the theory that cladding collapse can be detected by monitoring either the cladding elongation or the fuel centerline temperature. The LLR test data directly applicable to these theories consisted of data from one fuel rod. It is necessary, therefore, to review additional data and perhaps to gain a better understanding of the relationships between cladding collapse and elongation or centerline temperature before a correlation relating these parameters can be established. The steady-state data analysis also indicated that significant differences in cladding elongation and fuel centerline temperature measurements can be expected between identical fuel rods. To utilize these measurements to assess cladding deformation in LOFT will, therefore, require monitoring both parameters on a continuous basis to obtain data before and after the cladding collapse is suspected to have occurred for each instrumented fuel rod. In addition, power ramp rates must be controlled so as to eliminate ramp rate effects that complicate the elongation data.

As a result of the transient analysis, it is concluded that FRAP-T5 will predict cladding collapse before it actually occurs for a LOFT type fuel rod. The FRAP-T5 code would, therefore, provide a conservative evaluation of the condition and for the requalification of the LOFT core. The cladding deformation model in FRAP-T5 is a uniform collapse model, i.e., when the cladding deformation threshold is exceeded, the cladding is assumed to collapse uniformly onto the fuel pellet. Olsen's cladding deformation experiments show that caldding deformation varies in severity; initiated by two point contact (buckling), increasing to a uniform collapse (collapse) and finally plastic flow of the cladding (waisting). Thus, FRAP-T5 may predict the correct threshold for deformation but does not model the physical process correctly. Using Olsen's deformation data directly in LOFT cladding evaluation and requalification may provide a less conservative estimate of cladding deformation.

Finally, from the analysis to identify possible thermocouple effects from the relative centerline temperature response obtained from fuel rods with and without surface TCs, it is concluded that although the LLR test data may be indicative of the response expected if the surface thermocouples significantly changed the cooling characterisitcs at the rod surface, it is not possible to conclusively define a TC effect from these data. The analysis was based on centerline temperature instrumentation which gave unexplained anomalous centerline temperature data for one test and consequently the accuracy of all data from this instrumentation for the other tests must also be questioned. In addition, the analysis was based on the relative temperature response between the same two fuel rods and consequently the observed relative centerline temperature responses may actually be the result of, or complicated by, effects inherent to the fuel rods. It is noted, however, that the data do suggest a possible surface TC effect and probably warrants the review of additional data.

## 7. REFERENCES


1. D. J. Varacalle and R. W. Garner, PBF/LOFT Lead Rod Program Tests LLR-3, -4, -5 Quick Look Report, TFBP-TR-315, April 1979.

2. D. J. Varacalle and R. W. Garner, PBF/LOFT Lead Rod Program Test LLR-4A Quick Look Report, TFBP-TR-320, June 1979.

3. L. J. Siefken, et al., FRAP-T5--A Computer Code for the Transient Analysis of Oxide Fuel Rods, NUREG/CR-0840, TREE-1281, June 1979.

4. G. A. Reymann et al, MATPRO - Version 11: A Handbook of Materials Properties for Use in the Analysis of Light Water Reactor Fuel Rod Behavior, NUREG/CR-0497 TREE-1280 (February 1979).

5. 1976 ASHE Steam Tables, United Engineering Center, New York, NY.

6. G. B. Peeler, et al., Independent Assessment of Transient Fuel Rod Analysis Code FRAP-T5, EGG-CAAP-5074, December 1979.

7. D. E. Owen, Pellet-Cladding Mechanical Interaction in Halden Assembly IFA-226, NUREG/CR-0282, TREE-1266, August 1978.

8. J. R. Larson, et al., PBF-LOCA Test Series Test LOC-11 Test Results Report, NUREG/CR-0618, TREE-1319, April 1979.

9. M. L. Caroneau and E. L. Tolman, An Evaluation of the PBF LOFT Lead Rod Test Results Concerning Surface Thermocouple Perturbation Effects, LO-00-79-108, USNRC-P-394, February 1980.

10. C. S. Olsen, Zircaloy Cladding Collapse Under Off-Normal Temperature and Pressure Conditions, TREE-NUREG-1239, April 1978.